Aspects of Quantum Field Theory in Enumerative Graph Theory

by

Samuel Yusim

A thesis
presented to the University of Waterloo
in fulfillment of the
thesis requirement for the degree of
Master of Mathematics
in
Combinatorics & Optimization

Waterloo, Ontario, Canada, 2022

I hereby declare that I am the sole author of this thesis. This is a true copy of the thesis, including any required final revisions, as accepted by my examiners.

I understand that my thesis may be made electronically available to the public.

Abstract

While a quantum field theorist has many uses for mathematics of all kinds, the relationship between quantum field theory and mathematics is far too fluid in the world of modern research to be described as the simple provision of mathematical tools to physicists, as Feynman often framed it. Problems large and small of a seemingly purely mathematical nature often arise directly from a physical setting. In this thesis we focus on two combinatorial problems with deep physical motivations.

The first of these is the Quadrangulation Conjecture of Jackson and Visentin, which asks for a bijective proof of an identity relating numbers of maps to numbers of maps which are quadrangulations. We provide a set of auxiliary bijections culminating in a bijection between maps with marked spanning trees and chord diagrams with partitions of the chords into a non-crossing part and a 'genus-g' part, and a bijection between these partitioned chord diagrams and four-regular maps with marked euler tours.

The second problem comes from the CHY integral formulation of tree-level Feynman integrals in supersymmetric Yang-Mills theory, but amounts to the enumeration of ways to decompose 4-regular graphs into pair of edge-disjoint Hamiltonian cycles. We show that for any graph which is the edge-disjoint union of an arbitrary 2-regular graph and a cycle, there are at least $(n-2)!/4$ ways to decompose the result into two full cycles. Moreover, if the chosen 2-regular graph consists of only even cycles this bound improves to $(n-2)!/2$. Further, if the graph consists only of 2-cycles, we obtain the exact number of decompositions, which is $\frac{1}{2}(n-2)!!S_H^{\pm}(n/2-1,1)$, where $S_H^{\pm}(a,b)$ is the so-called signed Hultman number. Interestingly, this combinatorial problem turns out to have further connections to the study of genomic rearrangements in bioinformatics.

Acknowledgements

I am thankful to a great many people for helping me check and improve my writing, for helping me develop the ideas presented in this thesis, for helping me learn the enormous amount of background material required to place this research in its proper context, and for simply supporting me as I struggled to write this document.

Particular thanks go to Karen Yeats for advising me, and to Ilia Chtcherbakov, Justin Jaffray, and Forte Shinko for their extremely useful criticism.

Table of Contents

List of Figures

Chapter 1

Introduction

While a quantum field theorist has many uses for mathematics of all kinds, the relationship between quantum field theory and mathematics is far too fluid in the world of modern research to be described as the simple provision of mathematical tools to physicists, as Feynman often framed it. Problems large and small of a seemingly purely mathematical nature often arise directly from a physical setting. In this thesis we focus on two combinatorial problems with deep physical motivations.

In this chapter we begin by defining some basic notions from graph theory and the theory of combinatorial maps for the sake of self-consistency. Then an introduction to the basics of quantum mechanics and quantum field theory is provided in order to give some context for the reader who may be unfamiliar with this background material. Finally we provide some limited information on the moduli space $\mathcal{M}_{g,n}$ of complex curves of genus g with n marked points. This object is not studied directly in this thesis, but it is something of a focal point for all of the material covered, from the directions of both physics and mathematics.

Chapter 2 regards the Quadrangulation Conjecture of Jackson and Visentin, which asks for a bijective proof of an identity relating numbers of maps to numbers of maps which are quadrangulations. In genus zero, we give a set of bijections from maps with a marked spanning tree to quadrangulations with a marked Euler tour, to what we call medial strings, to chord diagrams partitioned into a pair of non-crossing subdiagrams, and back to maps. We generalize these bijections to genus g, where in particular the partitioned chord diagrams lift to chord diagrams with partitions of the chords into a non-crossing part and a 'genus-g' part.

Chapter 3 regards the problem of finding a lower bound to the number of so-called

compatible cycles to an arbitrary 2-regular graph. The motivation for this problem comes from the CHY integral formulation of tree-level Feynman integrals in supersymmetric Yang-Mills theory, but amounts to the enumeration of ways to decompose 4-regular graphs into pair of edge-disjoint Hamiltonian cycles. We show that for any graph which is the edge-disjoint union of an arbitrary 2-regular graph and a cycle, there are at least $(n-2)!/4$ ways to decompose the result into two full cycles. Moreover, if the chosen 2-regular graph consists of only even cycles this bound improves to $(n-2)!/2$. Further, if the graph consists only of 2-cycles, we obtain the exact number of decompositions, which is $\frac{1}{2}(n-2)!!S_H^{\pm}(n/2-1,1)$, where $S_H^{\pm}(a,b)$ is the so-called signed Hultman number. Interestingly, this combinatorial problem turns out to have further connections to the study of genomic rearrangements in bioinformatics.

1.1 Graphs and Combinatorial Maps

For self-consistency we provide some standard definitions and results about common concepts here. In what follows we choose slightly more complicated versions of the definitions one might see in [12], for example, in an effort to allow for our graphs to contain multiple edges between the same pair of vertices.

Definition 1.1.1. A *graph* is an ordered pair $G = (V, E)$ consisting of a set V and a multiset E of unordered pairs of elements of V. We often write $V(G)$ and $E(G)$ for the vertex- and edge-sets of G, and we often write $|G|$ for the number of vertices in G.

Definition 1.1.2. A *path* P in a graph G is a finite sequence $e_1, e_2, \ldots, e_k$ of edges in G for which e_i and e_{i+1} share a vertex for each i, and for which the vertex common to any pair of consecutive edges appears in no other edge of the sequence. The start and end of a path P are the vertex of e_1 which does not appear in e_2 and the vertex of e_k which does not appear in e_{k-1}, respectively. A *cycle* C in G is a path with an additional edge between its start and end. The *length* of a path or cycle is the number of vertices along that path or cycle.

Definition 1.1.3. A subset $S \subseteq E(G)$ is *connected* if there is a path from any vertex on an edge in S to any other. A *tree* T in a graph G is a connected subset of the edges of G which contains no cycles. A *spanning tree* is a tree for which every vertex is contained in at least one edge.

In the third chapter we will require the basics of matching theory, so we provide definitions following [12].

Definition 1.1.4. A *matching* M in a graph G is a subset of $E(G)$ with the property that no two edges in M share a vertex. A matching M is called *perfect* if every vertex of G is in an edge from M. A vertex in G is *saturated* in M if it appears in some edge of M.

Definition 1.1.5. A graph G is *bipartite* if its vertices can be partitioned into two disjoint sets A and B, with the property that any vertex in A is only adjacent to vertices in B and vice versa.

Proposition 1.1.6. A graph is bipartite if and only if it has no cycles of odd length.

Definition 1.1.7. In a bipartite graph G with a matching A, a path P is *alternating* if the edges of P are alternately in and not in A along P. In an arbitrary graph G with two edge-disjoint matchings A and B, a path P is AB-alternating if the edges of P are alternately in A and in B along P. Analogously we also discuss alternating and AB-alternating cycles.

Now we give some preliminary information about combinatorial maps [21] [18].

Definition 1.1.8. A *rooted map* is a 2-cell embedding of a graph in a surface, with a distinguished half-edge called the *root*. Henceforth, when we use the term 'map', we always mean rooted map. By '2-cell embedding' here we mean an embedding of the graph such that every face is homeomorphic to a 2-cell, i.e., an open disk.

Definition 1.1.9. A *submap* of a map G is a subgraph of the underlying graph whose inherited embedding is also a 2-cell embedding.

Definition 1.1.10. A *quadrangulation* is a (rooted) map with the property that a walk along the boundary of any face touches exactly four vertices (not necessarily distinct) before returning to its starting position. Note that this is slightly different from the condition that every face is bounded by four edges. The path on three vertices, for example, is a quadrangulation of the sphere despite not satisfying this second condition. C.f. figure 1.1.

Probably the most famous fact about graphs in surfaces, and one which we use heavily, is the following.

Theorem 1.1.11 (Euler's Formula)**.** For any map G with v vertices, e edges, and f faces in genus g,

$$v - e + f = 2 - 2g.$$

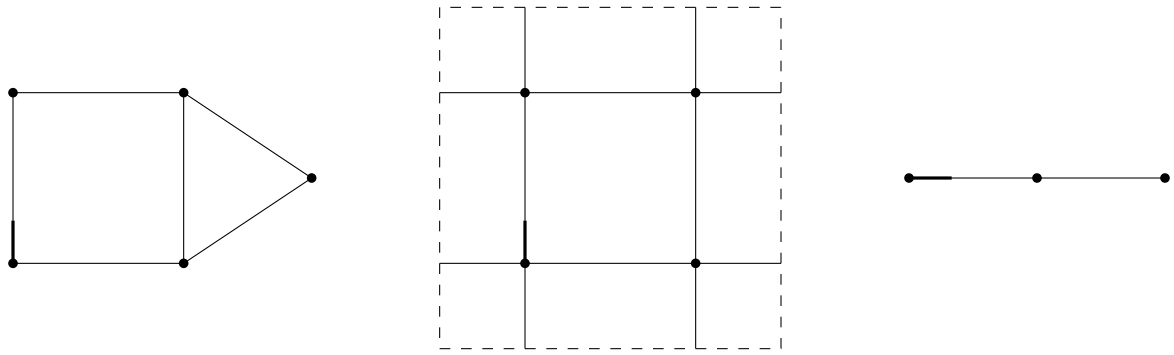

Figure 1.1: Left: a map in genus zero. Center: a quadrangulation in genus one. Right: a quadrangulation in genus zero. Roots are marked with a thicker edge segment.

An important piece of preliminary information is the notion of *rotation systems*. Given a map, three permutations can be constructed on the set H of half-edges. First, the permutation ν is constructed by recording the clockwise cyclic order of half-edges around each vertex. Second, the permutation ϵ is constructed by recording a transposition for every pair of half-edges that form an edge. Finally, the permutation ϕ is constructed by recording the outgoing half-edges from each vertex we hit along each facial walk, being sure to stay on the left of each edge as we walk along it in order to ensure the directions of these walks are coherent with each other.

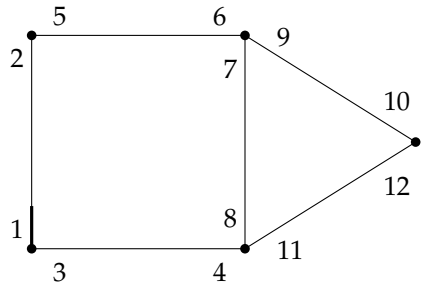

Figure 1.2: In this example map, we can read off the permutations of its rotation system:

$$\nu = (1\ 3)(2\ 5)(6\ 9\ 7)(8\ 11\ 4)(10\ 12)$$
$$\epsilon = (1\ 2)(3\ 4)(5\ 6)(7\ 8)(9\ 10)(11\ 12)$$
$$\phi = (1\ 5\ 9\ 12\ 4)(2\ 3\ 8\ 6)(7\ 11\ 10)$$

The following propositions are elaborated on in chapter 1.3.3 of [21].

Proposition 1.1.12. The permutations ν, ϵ, and ϕ uniquely determine a map, up to homeomorphism.

Proposition 1.1.13. For any map, we have $\nu\epsilon = \phi$.

As a consequence of these propositions, map enumeration (in orientable surfaces, so that walking on the 'left' as above is a sensible thing to do) amounts to a specific instance of a permutation enumeration problem. Observe that a map is also equivalent to the data of an abstract graph $G = (V, E)$ and a cyclic edge-incidence order around each vertex. Sometimes we refer to a pair of consecutive half edges around a vertex as an *angle*. As an aside, there is also a generalization of maps to non-orientable surfaces: we thicken every edge to a ribbon and track all four corners of each ribbon instead of both halves of each edge. This lets us track the additional information of whether an edge has been 'twisted'.

1.2 Quantum Mechanics and Quantum Field Theory

This section aims to very quickly bring a mathematician with little physics background up to speed with the basics of quantum mechanics and quantum field theory. This is necessary to explain the physical context for the material in this thesis. Such an undertaking has no doubt been done countless times, but it is still a worthwhile thing to do again, in the author's own words, and tailored to the particular direction the author intends to take the material described herein. In order to treat this material carefully from a mathematical standpoint we would need to use a significant amount of functional analysis, which we do not intend to do here. We take the view that the details of any analytic fact can be checked elsewhere, and we do not dwell on issues of convergence or well-definedness. The portion of this section focused on quantum mechanics follows [11] and the portion focused on quantum field theory follows [26].

From a mathematical standpoint, the key paradigm shift in physics that led to the development of quantum mechanics was to model a particle or physical system with a *state function*, which is a smooth, complex-valued function of position and time, with an additional property we shall provide shortly. We can consider these functions as elements of an infinite-dimensional complex Hilbert space with inner product

$$(\phi(\mathbf{x}, t), \psi(\mathbf{x}, t)) \mapsto \int_{\mathbb{R}^N} dx_1 \cdots dx_N \; \phi(\mathbf{x}, t)^* \psi(\mathbf{x}, t).$$

This inner product is often written in the so-called Dirac notation as $\langle\phi(t)|\psi(t)\rangle$. In this notation we also write $|\psi(t)\rangle := \psi(\mathbf{x}, t)$ and $\langle\phi(t)| := |\phi(t)\rangle^\dagger$ where $\dagger$ denotes the Hermitian conjugate. You will not go wrong if you think of this as being just like the conjugate-transpose in a finite-dimensional space. The additional property we require of an element $|\psi(t)\rangle$ of such a Hilbert space for it to be a state function is just that

$$\langle\psi(t)|\psi(t)\rangle = 1,$$

in other words that it be normalized.

A physicist would be interested in such an abstract construction because at a particular time t, if $S \subseteq \mathbb{R}^N$, then

$$\int_S dx_1 \cdots dx_N \psi^*(\mathbf{x}, t)\psi(\mathbf{x}, t)$$

is interpreted as the probability of finding the particle or physical system with state $\psi(\mathbf{x}, t)$ in the region S, and if $S = \mathbb{R}^N$ then this integral is just $\langle\psi(t)|\psi(t)\rangle = 1$: we can always find it *somewhere*. The abstraction becomes necessary for a physicist when experiment shows that particles are actually waves that don't exist in a specific place but rather across all of space.

The product $\psi(\mathbf{x}, t)^*\psi(\mathbf{x}, t)$ can be interpreted as a probability mass function of a random variable, a sampling of which gives a possible classical position of a particle or system described by ψ. ψ itself is often thought of as something like the square-root of a probability, whence it is termed a *probability amplitude*. For two state functions $\phi(\mathbf{x}, t)$ and $\psi(\mathbf{x}, t)$, there is also a physical interpretation of $\langle\phi(t)|\psi(t)\rangle$ at a particular time t: this is the probability amplitude of the state ψ producing a classical outcome which could also have been produced by the state ϕ.

Given a state $|\psi(t)\rangle$, a physicist wants to recover classical information like position, momentum, angular momentum, etc. To this end, let us consider some examples. Define the Hilbert space operator $\hat{X}$ by

$$\begin{aligned}\hat{X}\psi(\mathbf{x}, t) &= \mathbf{x}\psi(\mathbf{x}, t) \\ &= \begin{bmatrix} x_1\psi(\mathbf{x}, t) \\ \vdots \\ x_N\psi(\mathbf{x}, t) \end{bmatrix}\end{aligned}$$

$\hat{X}$ is typically called the *position operator*. The point of this definition is that

$$\langle\hat{X}\rangle_{\psi,t} := \langle\psi(t)|\hat{X}|\psi(t)\rangle = \int_{\mathbb{R}^N} dx_1 \cdots dx_N \mathbf{x}\psi(\mathbf{x}, t)^*\psi(\mathbf{x}, t)$$

(i.e., the N-dimensional vector whose jth component is $\int_{\mathbb{R}^N} dx_1 \cdots dx_n x_j \psi(\mathbf{x},t)^* \psi(\mathbf{x},t)$) which is interpreted as an expression for the *expected position* of $|\psi(t)\rangle$. It is the standard first example of a so-called *observable*. The next example is the *momentum operator* $\hat{p}$ defined by

$$\begin{aligned}\hat{p}\psi(\mathbf{x},t) &= -i\hbar\nabla\psi(\mathbf{x},t) \\ &= -i\hbar \begin{bmatrix} \frac{\partial}{\partial x_1}\psi(\mathbf{x},t) \\ \vdots \\ \frac{\partial}{\partial x_N}\psi(\mathbf{x},t) \end{bmatrix}\end{aligned}$$

and for which $\langle\hat{p}\rangle_{\psi,t} := \langle\psi(t)|\hat{p}|\psi(t)\rangle$ not-as-obviously gives an expression for the expected momentum. Both of these operators happen to have the property of being *Hermitian*, i.e., having all real eigenvalues, or equivalently having the property that $\hat{O} = \hat{O}^\dagger$. For a physicist it turns out that the terms 'Hermitian' and 'observable' are interchangeable.

As it happens, it is usually the case that

$$\langle\psi(t)|\hat{X}\hat{p}|\psi(t)\rangle \neq \langle\psi(t)|\hat{p}\hat{X}|\psi(t)\rangle.$$

The interpretation of this fact is that observing the position of some state has a non-negligible physical effect on any future observation of the momentum of that state, and *vice versa*. In other words, the fact that the commutator $[\hat{X},\hat{p}] \neq 0$ means that position and momentum *cannot* be observed simultaneously.

As another critical example, if we are looking at a state with a prescribed mass m, define the *kinetic energy operator* $\hat{T}$ by

$$\hat{T} = \frac{\hat{p}\cdot\hat{p}}{2m} = -\frac{\hbar^2}{2m}\nabla\cdot\nabla = -\frac{\hbar^2}{2m}\sum_{i=1}^{N}\frac{\partial^2}{\partial x_i^2}.$$

If we are given a particular system to describe, we will be able to determine some particular *potential energy operator* $V(\hat{X})$ for the particular physical system we are looking at. If we have such an operator we define the *Hamiltonian operator* $\hat{H} := \hat{T} + V(\hat{X})$, for which $\langle\hat{H}\rangle_{\psi,t} = \langle\psi(t)|\hat{H}|\psi(t)\rangle$ gives the total energy of the state ψ at the time t. If we have a system of n particles, we might write

$$\hat{H} = \sum_{i=1}^{n}\frac{\hat{p}_i\cdot\hat{p}_i}{2m_i} + V(\hat{X}_1,\ldots,\hat{X}_n) \tag{1.1}$$

decomposing the operator $\hat{T}$ into operators that each tell us the state of a specific individual particle in the system, and having V express the potential energy of the system in terms of each of the individual position operators. We might also decompose V into functions that describe interactions between pairs, triples, etc., of particles,

$$V(\hat{X}_1 \dots \hat{X}_n) = \sum_{i,j} k_{i,j} V(\hat{X}_i, \hat{X}_j) + \sum_{i,j,k} \ell_{i,j,k} V(\hat{X}_i, \hat{X}_j, \hat{X}_k) + \dots$$

The main mathematical engine of quantum mechanics amounts to choosing a particular function $V(\hat{X})$, and plugging it into the *Schrodinger equation*,

$$\hat{H}|\psi(t)\rangle = i\hbar \frac{\partial}{\partial t}|\psi(t)\rangle.$$

This will give a partial differential equation that can be solved for $|\psi(t)\rangle$, so that the particular choice of Hamiltonian forces a structure on the allowed states of the physical system. As it turns out, you can typically separate the variables $\mathbf{x}$ and t, writing $\psi(\mathbf{x}, t) = \psi(\mathbf{x})T(t)$, giving a pair of equations

$$\hat{H}\psi(\mathbf{x}) = E\psi(\mathbf{x}) \qquad \text{and} \qquad i\hbar \frac{\partial}{\partial t} T(t) = ET(t),$$

with E representing the total energy. The first of these is often called the *time-independent* Schrodinger equation, and the second has no dependence on the choice of V, and hence is always exactly the same, $T(t) = e^{iEt/\hbar}$. Therefore we can typically focus only on the time-independent equation. For particular values of E the time-independent Schrodinger equation is an eigenvalue equation! Depending on the particular properties of $V(\hat{X})$, the spectrum of $\hat{H}$ can take values in a continuum $[E_{\min}, \infty)$ or it can take only discrete values $\{E_n : n \in \mathbb{N}\}$. The latter phenomenon is called *quantization*.

Example 1.2.1. We shall solve the Schrodinger equation in one dimension with the potential $V(\hat{X})$ being a constant $V \in [0, \infty)$. In this case we have

$$\hat{H} = -\frac{\hbar^2}{2m}\frac{\partial^2}{\partial x^2} + V,$$

and we aim to first solve the partial differential equation

$$-\frac{\hbar^2}{2m}\frac{\partial^2}{\partial x^2}\psi(x,t) + V\psi(x,t) = i\hbar\frac{\partial}{\partial t}\psi(x,t).$$

Separate the variables, writing $\psi(x,t)$ as $\psi(x)f(t)$, and we will first solve the time-independent equation $\hat{H}\psi(x) = E\psi(x)$. To that end, plug in $\hat{T} + V(\hat{X})$ and rearrange to get

$$\frac{\partial^2}{\partial x^2}\psi(x) = -\frac{2m(E-V)}{\hbar^2}\psi(x)$$

and observe that a solution to this equation must take the form

$$\psi(x) = Ae^{ikx} + Be^{-ikx} \qquad \text{with} \qquad k = \frac{\sqrt{2m(E-V)}}{\hbar}.$$

If we require this to be normalized we can derive an algebraic relationship between A and B, but for the purposes of this document this is not worth doing.

In the last example, If $E < V$ then k is imaginary, and $\psi(x) = Ae^{ikx} + Be^{-ikx}$ becomes a sum of real exponentials. In the particular case we are working in where there are no bounds on the space we are looking at this cannot be allowed because these functions are unbounded and so cannot be normalized, but it we specify

$$V(x) = \begin{cases} 0 & x > 0 \\ V & x \leqslant 0 \end{cases},$$

then an exponential decay to the left is completely allowed for $x \leqslant 0$. This means that even though there would be no way for a particle to exist in this region in the classical picture, there is in fact a small chance of observing it there in the quantum picture.

Example 1.2.2. We shall solve the Schrodinger equation in one dimension with the potential

$$V(\hat{X}) = \begin{cases} 0 & x \in (-1,1) \\ \infty & \text{otherwise} \end{cases}.$$

This is known to physicists as an *infinite potential well*. Notice that if $|x| \geqslant 1$, we can solve for ψ in this region by taking the limit $V \to \infty$ from the constant case. If $x \leqslant -1$ then $\psi(x) = Be^{-ikx}$ with k positive-imaginary. As $V \to \infty$ we get $k \to i\infty$, which gives that $\psi(x)$ tends to the constant 0 function as $V \to \infty$ in this region. The case is similar for $x \geqslant 1$.

Now, in the region $(-1,1)$ we can use the first example again with $V = 0$, and since we require that ψ be continuous, we get the extra condition that $\psi(-1) = \psi(1) = 0$. This will force wavelength restrictions on $\psi(x) = Ae^{ikx} + Be^{-ikx}$, which amounts to only allowing a discrete set of energy levels. This is the typical first example of quantization.

Depending on the choice of Hamiltonian, the eigenvalue equation $\hat{X}|\psi(t)\rangle = \mathbf{x}|\psi(t)\rangle$ (more carefully, each coordinate of $\mathbf{X}$ gives us a different eigenvalue equation) might have a unique solution for particular $\mathbf{x}$, and in such a situation we would denote the symbol $|\mathbf{x}_0\rangle$ to be the state for which $\hat{X}|\mathbf{x}_0\rangle = \mathbf{x}_0|\mathbf{x}_0\rangle$. In general when we are working under an unspecified Hamiltonian the symbol $|\mathbf{x}_0\rangle$ just represents an arbitrary such state. We can do the exact same thing for any other observable. For $\hat{p}$, we might denote by $|p_0\rangle$ a state for which $\hat{p}|p_0\rangle = p_0|p_0\rangle$. If we take each $|x\rangle$ to be normalized, we find that they form an orthonormal basis for the infinite-dimensional Hilbert space of states, and the same is true for the $|p\rangle$. One can compute the coefficients for changing between these bases as

$$\langle \mathbf{x}|p\rangle = \frac{e^{i\mathbf{x}\cdot p}}{\sqrt{2\pi\hbar}}, \tag{1.2}$$

so that converting a vector $|\mathbf{x}\rangle$ into so-called *momentum space* can be done by computing

$$|\mathbf{x}\rangle = \int_{\mathbb{R}^N} dp_1 \cdots dp_N \langle \mathbf{x}|p\rangle |p\rangle$$

in analogy with the finite-dimensional change-of-basis formula $\mathbf{x} = (\sum_i \mathbf{x}\cdot\mathbf{y}_i)\mathbf{y}_i$.

Another linear algebraic fact we will make heavy use of is that, as operators,

$$\int dx_1 \cdots dx_N |\mathbf{x}\rangle\langle\mathbf{x}| = \int dp_1 \cdots dp_N |p\rangle\langle p| = \mathrm{id}, \tag{1.3}$$

where id is the identity operator. To see these in an informal way, think of how in a finite-dimensional vector space V with orthonormal basis $\{e_1, \ldots, e_n\}$, the sum of outer products $\sum_{i=1}^n e_i e_i^T$ is equal to the identity matrix.

Let us say more about how a state can evolve over time. We can give an operator, $U(t, t_0)$, defined by $U(t, t_0)|\psi(t_0)\rangle = |\psi(t)\rangle$. We can find an explicit form for $U(t, t_0)$ in terms of the Hamiltonian operator: we have

$$\hat{H}U(t, t_0)|\psi(t_0)\rangle = i\hbar\frac{\partial}{\partial t}U(t, t_0)|\psi(t_0)\rangle \qquad \Longrightarrow \qquad \hat{H}U(t, t_0) = i\hbar\frac{\partial}{\partial t}U(t, t_0)$$

and so

$$U(t, t_0) = e^{\frac{i(t-t_0)}{\hbar}\hat{H}} = \sum_{n=0}^{\infty} \frac{1}{n!}\left(\frac{i(t-t_0)}{\hbar}\right)^n \hat{H}^n$$

is the unique operator that satisfies this equation if we require that $U(t, t) = I$. A surprisingly important observation: $U(t, t_1)U(t_1, t_0) = U(t, t_0)$.

If we have an initial state $|\mathbf{x}_I\rangle$, we can compute the probability that it evolves to another state $|\mathbf{x}_F\rangle$ over a time interval t by computing the integral

$$\langle \mathbf{x}_F | \exp(it\hat{H}/\hbar)|\mathbf{x}_I\rangle = \int_{\mathbb{R}^N} dx_1 \cdots dx_N \psi_F(\mathbf{x})^* \exp(it\hat{H}/\hbar)\psi_I(\mathbf{x}),$$

where $|\psi_F\rangle$ and $|\psi_I\rangle$ are eigenstates of $\mathbf{x}_F$ and $\mathbf{x}_I$, respectively, under $\hat{X}$. For the sake of a thought experiment, if we place a barrier between our initial and final positions with tiny holes at positions $\mathbf{x}_1$ and $\mathbf{x}_2$, we get

$$\begin{aligned}\langle \mathbf{x}_F | \exp(it\hat{H}/\hbar)|\mathbf{x}_I\rangle = {} & \langle \mathbf{x}_F | \exp(it\hat{H}/2\hbar)|\mathbf{x}_1\rangle\langle \mathbf{x}_1 | \exp(it\hat{H}/2\hbar)|\mathbf{x}_I\rangle \\ & + \langle \mathbf{x}_F | \exp(it\hat{H}/2\hbar)|\mathbf{x}_2\rangle\langle \mathbf{x}_2 | \exp(it\hat{H}/2\hbar)|\mathbf{x}_I\rangle.\end{aligned}$$

If we have a large hole covering a region S in the barrier we would replace the sum with an integral, getting

$$\langle \mathbf{x}_F | \exp(it\hat{H}/\hbar)|\mathbf{x}_I\rangle = \int_S d^N\mathbf{x}\langle \mathbf{x}_F | \exp(it\hat{H}/2\hbar)|\mathbf{x}\rangle\langle \mathbf{x} | \exp(it\hat{H}/2\hbar)|\mathbf{x}_I\rangle,$$

and if there is no barrier at all, that should be the same as choosing $S = \mathbb{R}^N$ in this integral. Depending on your philosophy, this could be another reason for equation 1.3 to be true. Further, we can divide the time interval t into a large number n of equal segments δt and write

$$\begin{aligned}\langle \mathbf{x}_F | \exp(it\hat{H}/\hbar)|\mathbf{x}_I\rangle = \prod_{i=1}^{n}\left(\int_{\mathbb{R}^N} d^N\mathbf{x}_i\right)\langle \mathbf{x}_F | \exp(i\delta t\hat{H}/\hbar)|\mathbf{x}_1\rangle\langle \mathbf{x}_1 | \exp(i\delta t\hat{H}/\hbar)|\mathbf{x}_2\rangle \\ \cdots\langle \mathbf{x}_n | \exp(i\delta t\hat{H}/\hbar)|\mathbf{x}_I\rangle.\end{aligned}$$

For convenience we would like a closed form for the term $\langle \mathbf{x}_i | \exp(i\delta t\hat{H}/\hbar)|\mathbf{x}_{i+1}\rangle$. If potential energy is zero, we have

$$\begin{aligned}\langle \mathbf{x}_i | \exp(i\delta t\hat{H}/\hbar)|\mathbf{x}_{i+1}\rangle &= \int_{\mathbb{R}^N} d^N p\langle \mathbf{x}_i | \exp(i\delta t\hat{H}/\hbar)|p\rangle\langle p|\mathbf{x}_{i+1}\rangle && \text{(using equation 1.3)} \\ &= \int_{\mathbb{R}^N} d^N p e^{\frac{i\delta t p^2}{2m}}\langle \mathbf{x}_i|p\rangle\langle p|\mathbf{x}_{i+1}\rangle && (|p\rangle \text{ an eigenstate of } \hat{H}) \\ &= \frac{1}{2\pi\hbar}\int_{\mathbb{R}^N} d^N p e^{\frac{i\delta t p^2}{2m}} e^{ip(\mathbf{x}_{i+1}-\mathbf{x}_i)} && \text{(using equation 1.2).}\end{aligned}$$

This is a type of Gaussian integral, which we can evaluate. Not dwelling on it too much for now, the result is

$$\langle \mathbf{x}_i | \exp(i\delta t \hat{H}/\hbar) | \mathbf{x}_{i+1} \rangle = \left(\sqrt{\frac{-im}{2\pi\delta t}} \right)^N e^{\frac{im(\mathbf{x}_{i+1}-\mathbf{x}_i)^2}{2\delta t}}.$$

If from here we throw caution to the wind and let δt 'become infinitesimal' we can say

$$e^{\frac{im(\mathbf{x}_{i+1}-\mathbf{x}_i)^2}{2\delta t}} = e^{\frac{im\delta t}{2}\left(\frac{\mathbf{x}_{i+1}-\mathbf{x}_i}{\delta t}\right)^2} \longrightarrow_{n\to\infty} e^{\frac{im\,dt}{2}\left(\frac{d\mathbf{x}}{dt}\right)^2},$$

and then

$$\begin{aligned}\langle \psi_F | \exp(i\delta t \hat{H}/\hbar) | \mathbf{x}_1 \rangle \cdots \langle \mathbf{x}_n | \exp(i\delta t \hat{H}/\hbar) | \mathbf{x}_I \rangle &= e^{\sum_{i=0}^{n} \frac{im(\mathbf{x}_{i+1}-\mathbf{x}_i)^2}{2\delta t}} \\ &\longrightarrow_{n\to\infty} e^{\int dt \frac{1}{2} m \left(\frac{d\mathbf{x}}{dt}\right)^2}\end{aligned}$$

And, especially terrifyingly for a mathematician, a physicist will write

$$\int D\mathbf{x} := \lim_{n\to\infty} \prod_{i=1}^{n} \left(\int_{\mathbb{R}^N} d^N \mathbf{x}_i \right) \left(\sqrt{\frac{-im}{2\pi\delta t}} \right)^N$$

to give the expression

$$\langle \mathbf{x}_F | \exp(it\hat{H}/\hbar) | \mathbf{x}_I \rangle = \int D\mathbf{x} e^{\int dt \frac{1}{2} m \left(\frac{d\mathbf{x}}{dt}\right)^2},$$

known as the *Feynman path integral*. If we allow for a nonzero potential the numbers still go through (to the extent that they 'went through' in the first place) and we get

$$\langle \mathbf{x}_F | \exp(it\hat{H}/\hbar) | \mathbf{x}_I \rangle = \int D\mathbf{x} e^{\int dt \frac{1}{2} m \left(\frac{d\mathbf{x}}{dt}\right)^2 - V(\mathbf{x})}. \tag{1.4}$$

On the left we have the exponential of a Hamiltonian $\hat{H}$, and on the right we have the exponential of a Lagrangian $\mathcal{L} = \frac{1}{2} m \left(\frac{d\mathbf{x}}{dt}\right)^2 - V(\mathbf{x})$. The indefinite integral $S = \int dt \mathcal{L}$ is called the *action*.

Now we shall make one final abstraction, and we will have completely stepped out of the world of quantum mechanics and into the world of quantum field theory. We consider all of the particles of a particular type in the universe to manifest from a particular *quantum field* $\phi(\mathbf{x}, t) : \mathbb{R}^N \times \mathbb{R} \to \mathbb{R}^M$, a variation in which corresponds to the

presence of a particle. To adapt to this development we need to change the instances of position in equation 1.4 to be expressions in terms of ϕ. In analogy with equation 1.1, we do this by replacing the mass m with a mass per unit volume σ and writing

$$\frac{1}{2}m\left(\frac{d\mathbf{x}}{dt}\right)^2 \to \int_{\mathbb{R}^N} d^N\mathbf{x}\sigma\left(\frac{\partial\phi}{\partial t}\right)^2 \qquad \text{and} \qquad V(\mathbf{x}) \to V(\phi).$$

We would write the path integral in this case as

$$Z = \int D\phi e^{\int_0^t dt \int_{\mathbb{R}^N} d^N\mathbf{x}\sigma\left(\frac{\partial\phi}{\partial t}\right)^2 - V(\phi)} = \int D\phi e^{\int_0^t dt \int_{\mathbb{R}^N} d^N\mathbf{x}\mathcal{L}(\phi)},$$

and physicists are typically concerned with situations where V is a sum of a polynomial in ϕ and a $\nabla\cdot\nabla\phi$ term. Often this last is grouped with the $\left(\frac{\partial\phi}{\partial t}\right)^2$ and rewritten with the symbol $(\partial\phi)^2$, leaving $V(\phi)$ just a polynomial. Physicists are typically interested in situations where the action $S = \int dt\mathcal{L}$ has an explicit form in terms of ϕ which will make numerical calculation feasible.

We might be interested now in setting up an instance of this machinery which is as basic as possible in order to see what happens. We might choose to look at a *scalar* theory, i.e., one with $\phi : \mathbb{R} \to \mathbb{R}$, and a common first example would be $\mathcal{L} = \frac{1}{2}(\partial\phi)^2 - \frac{1}{2}m^2\phi^2 + \frac{\lambda}{4!}\phi^4$, the well-known ϕ^4-*theory*. There is no inherent dimension of space in which we need to work, and all of this material still holds together nicely without so much analytic baggage if we restrict to zero dimensions. If we focus on zero-dimensional spacetime, the density σ becomes a mass m again and the path integral just becomes an ordinary integral of the form

$$Z = \int_{-\infty}^{\infty} d\phi e^{S(\phi)}.$$

In the case of ϕ^4-theory in zero dimensions, the $\frac{1}{2}(\partial\phi)^2$ is zero because there's nothing to differentiate over, and this gives us a Gaussian integral

$$\begin{aligned}\int_{-\infty}^{\infty} d\phi e^{-\frac{1}{2}m^2\phi^2+\frac{\lambda}{4!}\phi^4} &= \int_{-\infty}^{\infty} d\phi e^{-\frac{1}{2}m^2\phi^2} e^{\frac{\lambda}{4!}\phi^4} \\ &= \sum_{n=0}^{\infty}\int_{-\infty}^{\infty} d\phi e^{-\frac{1}{2}m^2\phi^2}\frac{1}{n!}\left(\frac{\lambda}{4!}\phi^4\right)^n \\ &= \frac{\sqrt{2\pi}}{m}\sum_{n=0}^{\infty}\frac{1}{n!}\frac{\lambda^n}{4!^n}(4n-1)!!\end{aligned} \tag{1.5}$$

where the last equality comes from the fact that the kth moment of the Gaussian distribution is $(k-1)!! := 1 \cdot 3 \cdot 5 \cdots (k-1)$ if k is even and 0 otherwise. So if we ignore the extraneous $\sqrt{2\pi}/m$, it turns out after some manipulation that the path integral in this case is just an exponential generating function, and it turns out to count graphs with n 4-valent vertices, with labelled vertices and half-edges. These are the *Feynman diagrams* of this particular quantum field theory.

In the general case of a scalar quantum field theory, if the action is

$$S = -\frac{1}{2}m^2\phi^2 + \sum_{k=1}^{\infty} \frac{c_k x_k}{k!}\phi^k$$

for $c_k \in \{0,1\}$ for all k, we end up counting graphs (labelled as above) whose vertices have degrees exclusively from the set $\{k \in \mathbb{N} : c_k = 1\}$. For physical reasons, we typically write $x_1 = J$. In terms of graphs, the J term counts degree-one vertices, while for a physicist, Feynman integrals are often written

$$Z[J] = \int D\phi e^{\int dt \int d^N x \mathcal{L}(\phi) + J\phi} \tag{1.6}$$

for the same reason: the inclusion of the J term allows for the existence of sources and sinks of particles in an interaction.

Now let us circle around to a related mathematical problem, loosely following the presentation in chapters 3.1, 3.2, and 3.3 of [21]. Say we are interested in stratifying our enumeration of maps by genus. Using evocative symbols, let $T(N,s)$ be the exponential generating function for which the constant term is 1 and in the non-constant terms, $\frac{(2n-1)!!}{2}[N^k s^n]T(N,s)$ is the number of one-face maps with k vertices and n edges. The constant term and fractions are chosen to give the generating function the particularly nice form $T(N,s) = \left(\frac{s+1}{s-1}\right)^N$, a famous result of Harer and Zagier [25].

One way to calculate the coefficients of $T(N,s)$ goes as follows. First, let H be an $N \times N$ Hermitian matrix, and let $\mathcal{H}_N$ be the (N^2-real-dimensional) space of all Hermitian matrices, with real diagonal entries $h_{ii} = x_{ii}$ and complex off-diagonal entries $h_{ij} = x_{ij} + iy_{ij}$ such that $h_{ji} = h_{ij}^*$, the complex conjugate of h_{ij}. Let

$$d\nu(H) := \prod_{i=1}^{N} dx_{ii} \cdot \prod_{i<j} dx_{ij}\,dy_{ij},$$

the so-called standard measure, and let

$$d\mu(H) := \frac{1}{\sqrt{2\pi}^{N^2}} 2^{(N^2-N)/2} e^{-\frac{1}{2}\operatorname{tr}(H^2)} d\nu(H),$$

the Gaussian measure. For example, in the $N = 1$ case, if we set the mass m to 1 we can rewrite the integral 1.5 as

$$\sum_{n=0}^{\infty} \int_{-\infty}^{\infty} d\phi e^{-\frac{1}{2}m^2\phi^2} \frac{1}{n!} \left(\frac{\lambda}{4!}\phi^4\right)^n = \sum_{n=0}^{\infty} \sqrt{2\pi} \int_{-\infty}^{\infty} d\mu(\phi) \frac{1}{n!} \left(\frac{\lambda}{4!}\phi^4\right)^n.$$

Now for $f : \mathcal{H}_N \to \mathbb{C}$, write

$$\langle f \rangle_\mu := \int_{\mathcal{H}_N} d\mu(H) f(H).$$

This is the expected value of f with respect to the Gaussian measure.

Second, we give the following result on Gaussian expectations.

Theorem 1.2.3 (Wick's Theorem, theorem 3.2.5 of [21])**.** Let $f_1, \ldots, f_{2n}$ be degree-one polynomials in the x_{ii}, x_{ij} and y_{ij}. Then

$$\langle f_1 f_2 \cdots f_{2n} \rangle_\mu = \sum \langle f_{p_1} f_{q_1} \rangle_\mu \langle f_{p_2} f_{q_2} \rangle_\mu \cdots \langle f_{p_n} f_{q_n} \rangle_\mu$$

where the sum is taken over all permutations of $1, 2, \ldots, 2n$ with a one-line notation expression of the form $p_1 q_1 p_2 q_2 \ldots p_n q_n$ where $p_1 < p_2 < \ldots < p_n$ and $p_i < q_i$ for all $i \in \{1, \ldots, n\}$. In other words, the sum is over all the distinct ways of pairing the f_i, and we place a natural ordering on the indices of the f_i when we write any particular term. There are $(2n-1)!!$ terms in the sum.

It should be noted that $(2n-1)!!$ is also the number of rooted chord diagrams with n chords, since every choice of a pair of endpoints to place a chord between lowers the number of remaining endpoints by two.

We also remark that for $H = (h_{ij}) \in \mathcal{H}_N$, we have

$$\langle h_{ij} h_{kl} \rangle_\mu = \begin{cases} 1 & kl = ji \\ 0 & kl \neq ji \end{cases}$$

and if f is a polynomial in the h_{ij} of odd degree then $\langle f \rangle_\mu = 0$.

Third, we observe that because the $h_{ij} = x_{ij} + iy_{ij}$ are indeed degree-one polynomials in the x_{ij} and y_{ij}, we can write

$$\langle \operatorname{tr} H^n \rangle_\mu = \sum_{i_1, i_2, \ldots, i_n = 1}^{N} \langle h_{i_1 i_2} h_{i_2 i_3} \cdots h_{i_{n-1} i_n} h_{i_n i_1} \rangle_\mu$$

and apply Wick's theorem. In a particular term of the Wick sum, if $h_{i_k i_{k+1}}$ and $h_{i_\ell i_{\ell+1}}$ get paired, then for the contribution of the summands containing $\langle h_{i_k i_{k+1}} h_{i_\ell i_{\ell+1}} \rangle_\mu$ to be nonzero we must have $i_k = i_{\ell+1}$ and $i_{k+1} = i_\ell$. If the identifications made by the pairs leave us with k degrees of freedom in choosing the $i_1, \ldots, i_n$ we will get a contribution of N^k from those terms in the trace sum. So $\langle \operatorname{tr} H^n \rangle_\mu$ is a polynomial in N.

Fourth, we interpret the polynomial $\langle \operatorname{tr} H^n \rangle_\mu$ combinatorially. For n even, imagine an n-gon with vertices labelled i_1 through i_n, going clockwise around. The different ways of gluing the sides $i_k i_{k+1}$ of the n-gon together will correspond to different terms in the Wick sum. The resulting surface will be orientable, since we can only make identifications $i_k = i_{\ell+1}$ and $i_\ell = i_{k+1}$, rather than $i_k = i_\ell$ and $i_{k+1} = i_{\ell+1}$. Moreover, the obtained surface with the identified sides and vertices on it will constitute a map with one face. If a term contributes N^k in the trace sum, the map obtained by the corresponding side identification will have k vertices. Because we started with an n-gon, we know the map will have $n/2$ edges. This means we can isolate terms with a specific genus by picking n and k such that $k - n/2 + 1 = 2 - 2g$ for our desired g, and computing all of the $\langle \operatorname{tr} H^n \rangle_\mu$ that we want.

In summary, the second variable we needed for our generating function came out of the sizes of the matrices we were looking at when we generalized the Gaussian integral calculation from scalars to Hermitian matrices of arbitrary sizes. One can extend these computations to arbitrary graphs with face degrees $f_1, \ldots, f_k$ by computing $\langle \prod_{i=1}^{k} \operatorname{tr} H^{f_i} \rangle_\mu$. One could recover an expression for maps by putting these into a generating function and reducing to the connected case by taking a logarithm in the usual way.

Now let us briefly return to the Feynman path integral, this time in the positive-dimensional case. The graph-enumerative structure still appears here, but in contrast with the zero-dimensional scenario the $\frac{1}{2}(\partial\phi)^2$ from the Lagrangian and the integral in the exponential do not disappear and so for every graph we obtain a finite-dimensional integral to compute. If the particular quantum field theory we work with is well-behaved then the magnitude of the integral for a graph will quickly shrink with an increase in some graph-theoretic parameter such as the number of vertices or the number of cycles in the graph (known to physicists as *loops*), and so we can estimate the true value of the path integral with a finite computation. Later in this thesis, the theory of the contribution of trees to a certain class of Feynman integrals is the main motivation for posing one of the problems we solve.

1.3 The Moduli Space of Curves

The goal of this section is merely to provide some context from the wider mathematical world for the content of this thesis. While map enumeration is a relatively down-to-earth subject, it turns out to lie at the heart of one of the most strikingly broad areas of mathematics. The combinatorial treatment of Gaussian integrals from the last section originally appeared in [25] in the context of computing the Euler characteristic of $\mathcal{M}_{g,n}$. The following short barrage of definitions [21] is necessary, although the details of these definitions are not particularly important for us.

Definition 1.3.1. A *complex curve* X is a connected complex manifold of complex dimension 1, in other words, it is a connected manifold with charts $U \to \mathbb{C}$ for open subsets $U \subseteq X$. As with real manifolds, we call X *smooth* when for any two open subsets $U, V \subseteq X$ with charts $\phi : U \to \mathbb{C}$ and $\psi : V \to \mathbb{C}$, the restrictions to $U \cap V$ have the property that $\phi \circ \psi^{-1} : \mathbb{C} \to \mathbb{C}$ is holomorphic.

Definition 1.3.2. A *holomorphism* between two complex curves X_1 and X_2 is a map $f : X_1 \to X_2$ such that for any $p \in X_1$ there is a neighbourhood U of $p \in X_1$ with a chart $\phi : U \to \mathbb{C}$ and a neighbourhood V of $f(p) \in X_2$ with a chart $\psi : V \to \mathbb{C}$ such that $\psi \circ f \circ \phi^{-1} : \mathbb{C} \to \mathbb{C}$ is holomorphic at p. Two complex curves X_1 and X_2 are *biholomorphically equivalent* if there is an invertible holomorphism $f : X_1 \to X_2$ with a holomorphic inverse.

Definition 1.3.3. A *ramified covering* of the Riemann sphere $\mathbb{C}P^1$ is a compact complex curve X with a holomorphic function $\phi : X \to \mathbb{C}P^1$ endowing it with the structure of a covering space, except at a finite number of points, known as the *ramification points*. If S is the set of ramification points, a *sheet* is a connected component of the preimage $\phi^{-1}(\mathbb{C}P^1 \setminus S)$. If the covering has k sheets away from the ramification points, a ramification point with a fibre of size $k-1$ is called *simple*.

If we imagine a ramified cover of $\mathbb{C}P^1$ with some particular number k of sheets away from the ramification points, we find that starting on the ith sheet and travelling, say, clockwise, around a particular ramification point for one full turn will take us to the jth sheet. In this way we recover a permutation σ_p for each ramification point p. A permutation arising from a simple ramification point must be a transposition.

One of the most important external motivations for studying the enumeration of maps is its application to the problem of computing *Hurwitz numbers* $h_{g,n}$. These are the numbers of ramified coverings of the Riemann sphere by a surface of specified genus g with non-simple ramification at one point, which we take to be ∞, and with the fibre of

∞ having n elements, up to biholomorphic equivalence. The *Riemann-Hurwitz formula* is a statement about more general ramified coverings which in the case of Riemann sphere coverings with one non-simple ramification point states that such a covering must have $n + k + 2g - 2$ additional simple ramification points, and that the group generated by their corresponding transpositions τ_i, for $i = 1, \ldots, n + k + 2g - 2$, must act transitively on the set of sheets. It also happens that for any such covering,

$$\left(\prod_{i=1}^{n+k+2g-2} \tau_i \right) \cdot \sigma_\infty = \mathrm{id}\,.$$

Up to biholomorphic equivalence the permutation σ_∞ and the transpositions τ_i completely determine the covering. Hence both the computation of Hurwitz numbers and the enumeration of maps have interpretations as particular permutation-factorization enumeration problems.

If we take a basepoint $x_0 \in \mathbb{C}P^1$ away from any of these ramification points, the preimage of a curve drawn from x_0 to ∞

Definition 1.3.4. The *moduli space of curves of genus* g *with* n *marked points*, denoted $\mathcal{M}_{g,n}$ is the set of compact smooth complex curves of genus g with n marked points, taken up to biholomorphic equivalence. A precise definition of the topology on this set would take us far beyond the scope of this thesis. An element of $\mathcal{M}_{g,n}$ is written $(X; x_1, \ldots, x_n)$.

It is a famous result [13] that the Hurwitz number $h_{g,n}$ can be computed as a particular integral over the compactified moduli space $\overline{\mathcal{M}_{g,n}}$, which is not unlike a Feynman integral.

Chapter 2

A Cycle of Bijections With Application to the Quadrangulation Conjecture

2.1 Background

2.1.1 Bijective Proofs

This chapter is focused on the notion of a 'bijective proof' of an equation. For any unfamiliar readers we begin with a brief example.

Given an integer equation to prove, we can do so by constructing two sets of sizes given by the left and right sides of the equation and constructing a bijective function between the two sets. As an archetypical example, we can show $2\binom{n}{2} = n(n-1)$ by writing down the sets $A = \{0,1\} \times \{(a,b) : a,b \in \{1,\dots,n\}, a > b\}$ and $B = \{1,\dots,n\} \times \{1,\dots,n-1\}$, noting that $|A| = 2\binom{n}{2}$ and $|B| = n(n-1)$, and then showing by constructing a bijection that $|A| = |B|$. To complete this example, consider the function $f : A \to B$ given by

$$(q,(a,b)) \mapsto \begin{cases} (a,b) & q = 0 \\ (b+1,a) & q = 1, a \neq n \\ (1,b) & q = 1, a = n \end{cases}.$$

One can see that f is injective since $a > b$ means a can never be 1, and it can be verified using a case analysis on the elements of B that f is surjective: let $(x,y) \in B$. If $x > y$, then (x,y) is the image of $(0,(x,y))$, etc. Often we are instead interested in showing a

function is a bijection by constructing a second function which we would show is the two-sided inverse of the first.

2.1.2 The Quadrangulation Conjecture

Let $Q(u^2, x, y, z)$ and $M(u^2, x, y, z)$ be the generating functions for maps which are quadrangulations, and all maps, respectively, where the powers of u^2 mark genus, and powers of x, y, and z mark the numbers of vertices, edges, and faces, respectively. It is a result of Jackson and Visentin [16] [18] that

$$Q(u^2, x, y, z) = \frac{1}{2}M(4u^2, x - u, y, xz^2) + \frac{1}{2}M(4u^2, x + u, y, xz^2).$$

The proof they give of this fact makes heavy use of the character theory of symmetric groups. Extracting coefficients gives the following result.

Proposition 2.1.1.

$$q(g, 2e) = \sum_{\gamma=0}^{g} \sum_{f=1}^{\infty} 2^{2\gamma} \binom{f}{2g - 2\gamma} a(\gamma, f, e),$$

where quadrangulations are specified by their genus and number of edges, since the number of faces and vertices are then determined by Euler's formula, and similarly for all maps if the numbers of faces and edges are specified.

Since this formula has been stated in many places but to the author's knowledge has never been explicitly derived in the literature, we shall do so here. Essentially it amounts to writing down an explicit generating function for M and Q and manipulating the two series in a standard way.

Proof. Begin by writing $M(u^2, x, y, z) = \sum_{g,f,e} a(g, f, e) u^{2g} x^{\nu} y^e z^f$, where $\nu := 2 - 2g + e - f$ by Euler's formula. Now,

$$\begin{aligned} M(4u^2, x \pm u, y, xz^2) &= \sum_{g,f,e} a(g, f, e) 2^{2g} u^{2g} y^e x^f z^{2f} \sum_{k=0}^{\nu} (\pm 1)^k \binom{\nu}{k} x^k u^{\nu - k} \\ &= \sum_{g,f,e} \sum_{k=0}^{\nu} a(g, f, e) (\pm 1)^k 2^{2g} \binom{\nu}{k} u^{2g + \nu - k} x^{f + k} y^e z^{2f} \end{aligned}$$

So in the expression $F := \frac{1}{2}M(4u^2, x-u, y, xz^2) + \frac{1}{2}M(4u^2, x+u, y, xz^2)$, we will have terms with odd k cancelling, leaving only the even terms. We get

$$Q = \sum_{g,f,e} \sum_{k=0}^{\lfloor \nu/2 \rfloor} a(g,f,e) 2^{2g} \binom{\nu}{2k} u^{2g+\nu-2k} x^{f+2k} y^e z^{2f}.$$

Since Q is a generating function for quadrangulations, which are the duals of 4-regular maps, we also know by the handshake lemma on the duals that $4f = 2e$, i.e., $e = 2f$. Now if we extract the coefficient $[u^{2\alpha} y^{2\beta}] Q(u^2, x, y, z)$, we will find that as the sum over k runs from $k = 0$ to $\lfloor \nu/2 \rfloor$, the genus $2g$ will range in increments of two from $2\alpha - \nu$ to $2\alpha - \nu + 2\lfloor \nu/2 \rfloor = 2\alpha$. Equivalently, by rearranging the equations $2g = 2\alpha - \nu, \ldots, 2g = 2\alpha$, we will have a sum with 2α ranging from $2g - \nu$ to $2g$. Applying this reindexing and the handshake lemma will give the result. □

The so-called *quadrangulation conjecture*, or 'q-conjecture', is not so much a conjecture but an open problem: construct a bijective proof of the above identity.

Well-known in the literature regarding the quadrangulation conjecture [2][20] is the so-called *medial construction*. This is a natural bijection for the genus-zero case, but it does not generalize in an obvious way to higher genera.

Definition 2.1.2. Given a map G, the *medial graph* (or *medial map*) of G is the graph $M(G)$ obtained by adding a vertex to every face f, connecting the f-vertex to each vertex bounding f, and deleting the original edges of the graph.

Observe that any edge in the original map is bounded by a unique quadrangle in the medial graph, which itself can be shown to be a well-defined map since it naturally inherits a cyclic edge incidence order at each vertex. These boundaries of the old edges are all of the faces of the new map, and so we get a quadrangulation. It is worth clarifying that in the literature either $M(G)$ or its dual map are considered the medial map, depending on the author's preference. The dual can be realized in a more straightforward way by placing a vertex halfway along each edge, and then connecting these once for each facial walk which hits one and then the other.

In the plane, we can also go the other way in this construction, since we can 2-colour the vertices and then connect the black ones by an edge in a new map if they share a face in the old map. Swapping the colours here gives the dual map. If we turn to higher genera, though, we find that there is more ambiguity than we hoped.

There are a few more auxiliary concepts to record some basic information about before we move on to the results.

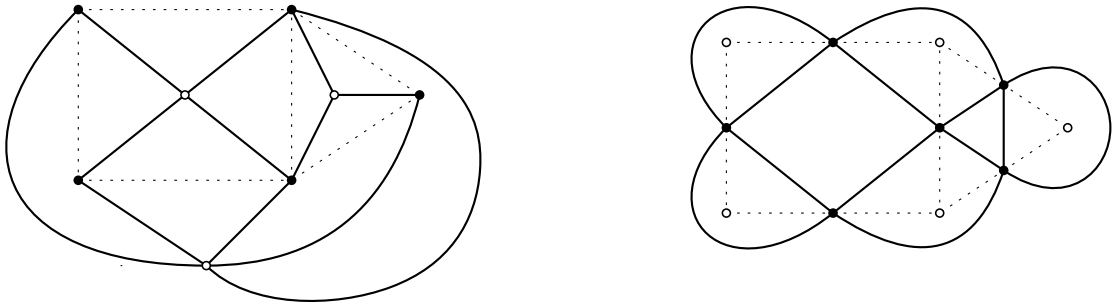

Figure 2.1: Left: A plane map (dashed edges) along with its medial map (solid edges). Right: a construction of the dual medial map directly from the original.

Definition 2.1.3. An *Euler tour* in a graph G is a path that touches every edge and returns to its starting vertex.

Theorem 2.1.4 ([12])**.** A connected graph G admits an Euler tour if and only if every vertex of G has even degree.

Proof. ($\Longrightarrow$) If some vertex has odd degree, then it is impossible for the tour to exit that vertex from a unique edge for every time it is entered.

($\Longleftarrow$) Assume that G has all even degrees and is a smallest counterexample. Then let W be a longest-possible walk in G that hits every edge at most once. Since G is connected and assumed not to admit an Euler tour, this walk must miss at least two edges at some vertex v which is hit by W. Now, in the graph $G \setminus W$, the connected component of v must have all even degrees, and since it is smaller than G we know by assumption that it admits an Euler tour. But we can append this tour to W at any point where it hits v to get an even longer tour in G that hits every edge at most once, which is a contradiction. □

The layout of the remainder of this chapter is as follows. Section 2 will discuss a cycle of correspondences between various combinatorial objects, including genus-zero maps and genus-zero quadrangulations, proving correctness of each. These are all known to different groups of researchers within the broad field of combinatorics, but to our knowledge have never been put together. Additionally we track some new special substructures through the correspondences and find that they have natural realizations at each stage. Section 3 will discuss generalizations of this cycle of bijections to higher genera. The reasoning for this approach is that if we factor one correspondence into several, then each part will individually be easier to bring to arbitrary genus.

2.2 The Correspondence Cycle

We begin by laying out the set of correspondences to be constructed. We first give a correspondence between marked quadrangulations and non-crossing Eulerian tours thereof. Next, we show that these can be made into chord diagrams, and then that the chord diagrams correspond to maps with marked spanning trees. Finally, we will show that the medial construction will turn the resulting map into the original quadrangulation.

2.2.1 Quadrandulations and Euler Tours

We start with a 2-vertex-coloured quadrangulation. We may consider the same colouring as a 2-face-colouring on the dual in the natural way. For now we will focus on showing that a quadrangulation has the necessary structure for our construction to be well-defined. We additionally take our quadrangulation to have a distinguished spanning tree, and we observe how this additional structure is translated through the different correspondences.

Lemma 2.2.1 ([14])**.** The dual of any planar quadrangulation admits a non-crossing Euler tour.

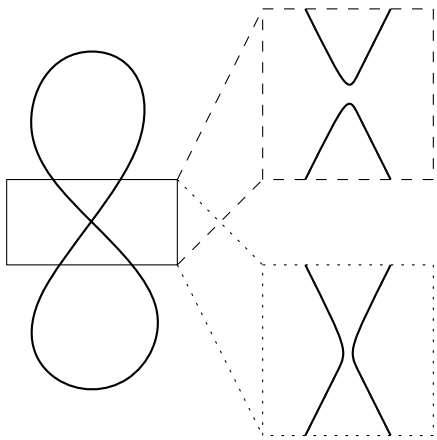

Figure 2.2: At least one way of resolving any crossing must not disconnect the tour.

Proof. It is a standard result that every connected graph whose degrees are all even admits some Euler tour. Since 4 is even, this result applies in our case. From here we will show that any Euler tour gives rise to a non-crossing one. So, assume there is at least one such crossing, at a vertex v. If the tour has the form $\ldots a v b \ldots c v d \ldots$, then we may redirect the tour as $\ldots a v c \ldots b v d \ldots$ with the segment between b and c reversed from the original tour. By induction on the number of crossings, we have the result. □

Given this result, we know that there is a non-crossing Euler tour of the dual of any medial graph. Moreover, if we track the correct information we can actually get a canonical tour. In particular, if we mark vertices in this dual-medial map which correspond to a spanning tree in the original map, we get a turning rule for a walk: at a marked vertex, stay in the light face of the current edge, and on an unmarked vertex, stay in the dark face of that edge.

We do not know *a priori* that these rules always give Euler tours, though, so we must prove that this is the case.

Lemma 2.2.2. The turning rule described above always gives an Euler tour on dual-medial maps with markings given by a spanning tree of the original map.

Proof. Observe first that the edges of the dual-medial map correspond to the angles between the edges in the original map. Second, notice that if we walk around a spanning tree for a map, we hit every such angle. Third, recording the angles in the order they are hit gives the desired tour. The unmarked vertex rule corresponds to turning across an edge in the original map while staying on the same vertex, and the marked vertex rule corresponds to walking to the next vertex in the spanning tree. □

Definition 2.2.3. Say we are given an Euler tour in the form of a cyclic string up to rotation, whose alphabet is the vertex set of a graph, which contains each letter twice, and with the letters of the string containing the additional information that the string is 2-coloured with the colouring coming from marking presence in a spanning tree in the original map, and that both instances of each letter will always have the same colour. For conciseness, we shall call a cyclic string so obtained *medial*.

We must show that all of the above information can be recovered. We first want to be able to naively draw a map out of the string. A given medial string does not necessarily represent a unique Euler tour, but the following result shows that it does represent a unique *non-crossing* Euler tour.

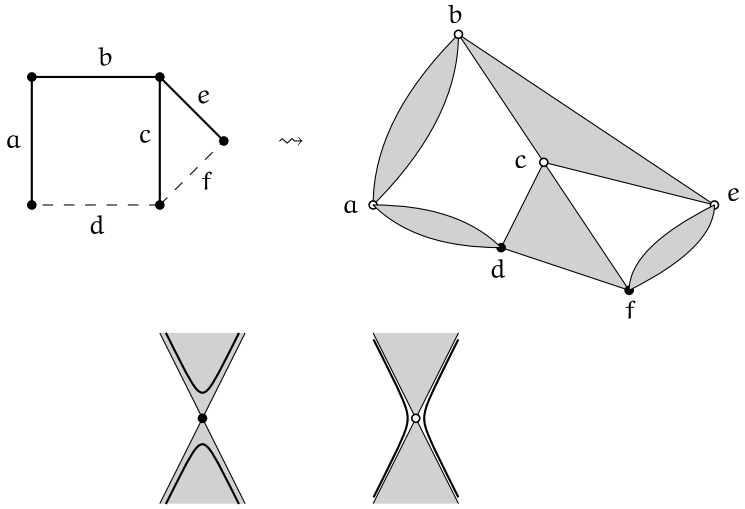

Figure 2.3: Top: an example of a labelled 2-coloured dual-medial map obained from a map with a labelled spanning tree. Bottom: the turning rules. In the example from the top figure we obtain the tour $abefecfdcbad$.

Proposition 2.2.4. Every medial cyclic string is a non-crossing Euler tour of a unique 4-regular map with marked vertices.

Proof. We begin with existence. Let the Euler tour be given by the cyclic string $S = v_1 v_2 \dots v_{2k}$. We will construct the map by constructing its rotation system. We will use the symbols $e_{i,0}$ and $e_{i,1}$ to denote the half-edges traversed as we pass through v_i. Then the edge permutation can be given in cycle notation as

$$\eta = (e_{1,1}\ e_{2,0})(e_{2,1}\ e_{3,0}) \cdots (e_{2k-1,1}\ e_{2k,0})(e_{2k,1}\ e_{1,0}).$$

Next, we construct the vertex permutation. We know that every letter in S appears exactly twice, so there exists a function $f : [2k] \to [2k]$ which sends i to the position of the other instance of v_i. Indeed, f is an involution. Since the tour is non-crossing, we know that, clockwise around a vertex v_i, the half edges must be arranged as one of the following four choices, as in figure 2.4:

$$(e_{i,0}\ e_{i,1}\ e_{f(i),0}\ e_{f(i),1}) \qquad (e_{i,1}\ e_{i,0}\ e_{f(i),0}\ e_{f(i),1})$$
$$(e_{i,0}\ e_{i,1}\ e_{f(i),1}\ e_{f(i),0}) \qquad (e_{i,1}\ e_{i,0}\ e_{f(i),1}\ e_{f(i),0})$$

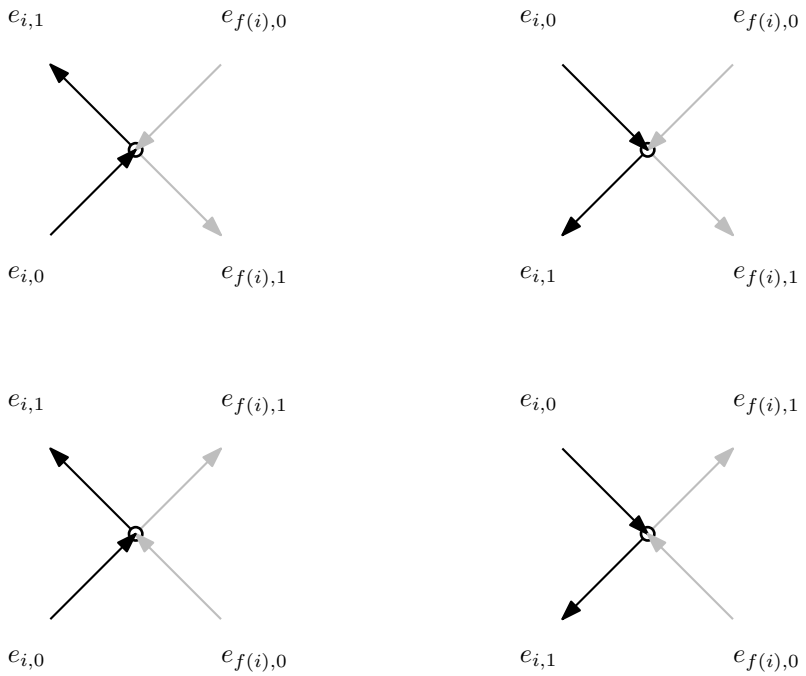

Figure 2.4: An illustration of the four possible configurations of a vertex.

Now, since f is an involution and we make no distinction between i and $f(i)$, it is plain to see that the first and last of these four configurations are equivalent. The case is similar for the second and third configurations. The choice of which one of the two cycles we use to record the order around a vertex comes down to the spanning tree turning rule, so we are done. □

Lemma 2.2.5. Removing both instances of any letter from a medial cyclic string with at least two distinct letters produces another medial cyclic string.

Proof. Let S be a medial cyclic string containing the letter S. Let a be a letter in S, and let $\hat{S}$ be the string S with both instances of a removed. We know by proposition 2.2.4 that S is an Euler tour in some 4-regular map G. For a nontrivial string S there are two cases: either the two instances of a are adjacent or they are not. If they are adjacent, S has the form $\ldots xaay\ldots$ with x and y not necessarily distinct. Then construct the map $\hat{G}$ by deleting the vertex a and all incident edges, and inserting the edge xy. On the other hand, if the two instances of a are not adjacent in S, then S has the form $\ldots xay\ldots zaw\ldots$, with x, y, z, and w not necessarily distinct. In this case, construct the

map $\hat{G}$ by deleting the vertex a and all incident edges, and adding edges xy and zw. It is clear in both cases that $\hat{G}$ is a 4-regular map and that $\hat{S}$ is a non-crossing Euler tour of $\hat{G}$, so by another application of proposition 2.2.4, we are done. □

2.2.2 Euler Tours and Chord Diagrams

Definition 2.2.6. A *chord diagram* is a finite set S with a cyclic order and a partition of S into subsets of size two. The size-two subsets of S are called *chords*, and we typically represent chord diagrams as a drawing of a disc with several lines, possibly crossing, drawn inside of the disc, so that no two such lines begin or end at the same point along the disc.

Definition 2.2.7. A *crossing* in a chord diagram is a pair of chords $\{a, b\}$ and $\{c, d\}$ such that in the cyclic order along S, the symbols appear in the order a, c, b, d. A chord diagram is said to be *non-crossing* if it contains no crossings.

An Euler tour of a 4-regular map can be represented by a cyclic word in the vertices of the graph which contains every vertex twice. We can obtain a chord diagram by writing this word around a $2|V|$-gon and drawing chords between vertices with the same label, and having the chords inherit the vertex colouring from the tour. On the other hand, if we are given a chord diagram with two edge colours, labelling the ends of each chord with matching symbols produces a cyclic sequence of letters satisfying the hypotheses of proposition 2.2.4, and thus describes an Euler tour of some 4-regular map.

Proposition 2.2.8. The inherited colouring on the chords partitions the chord diagram into two non-crossing subdiagrams.

Proof. Say two chords a and b of the same colour are crossing. By repeatedly applying lemma 2.2.5 to every letter besides a and b, we can assume that the cyclic string is exactly $abab$, whose 4-regular graph must be the banana on 4 edges. Since a and b are assumed to be the same colour, we would have that there is a non-crossing Euler tour of the 4-edge banana where we only turn, say, clockwise at every vertex. This is impossible, so we have achieved the desired contradiction. □

The 4-regular map can also be recovered by drawing all of the chords of one colour on the outside of the disc and all of the chords of the other colour on the inside of the disc, and then contracting all the chords into vertices. The underlying graph can be recovered by contracting the chords without this intermediate step.

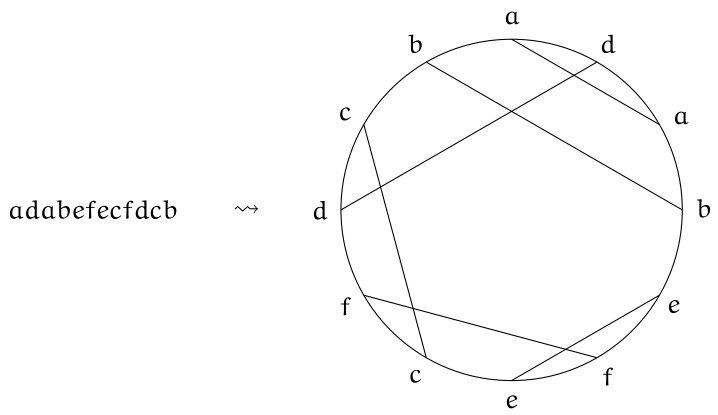

Figure 2.5: An example of a chord diagram obtained from a medial cyclic string.

2.2.3 Chord Diagrams and Maps

Given a chord diagram which can be partitioned into two sets of non-crossing chords, we now aim to demonstrate that this structure also uniquely corresponds to a planar map when obtained as above, with the partition corresponding to a choice of spanning tree. Further, we aim to demonstrate that this correspondence is equal to the composition of the correspondences in the last several sections. We begin by showing that a chord diagram with a partition into two sets of non-crossing edges generates a unique planar map with a marked spanning tree.

Lemma 2.2.9. Given a map G of genus 0, the set of one-face submaps of G touching every vertex is exactly the set of spanning trees of G.

Proof. Let H be a one-face submap of G containing every vertex of G. Then by Euler's formula applied to H, and since we are in genus zero,

$$|V(H)| - |E(H)| + |F(H)| = 2$$

but since $V(H) = V(G)$ and $|F(H)| = 1$, we get

$$|E(H)| = |V(G)| - 1.$$

Since H has one face, we also know it has no nontrivial cycles, and so we obtain the desired result.

On the other hand, say that T is a spanning tree of G. Then since T is acyclic, we know it has one face, and since G had genus zero, we know that T is indeed a submap of G, since its face is homeomorphic to a disc. □

As a bit of foreshadowing, be careful that in higher genera, a spanning tree is not a submap because its one face is not homeomorphic to a disc.

Proposition 2.2.10. Let C be a chord diagram and M be a set of non-crossing chords in C with the property that the chord diagram $C \setminus M$ is also non-crossing. Then the pair (C, M) uniquely corresponds to a planar map with a marked spanning tree.

Proof. To achieve the result we must draw the chord diagram in the plane as follows: first, we draw the chord diagram $C \setminus M$ in the standard way, recognizing that this drawing also specifies a 3-regular planar map, which we label G_C. Now, we create a sort of dual map $\widehat{G}_C$ by placing a vertex in each bounded region of G_C and connecting these by an edge if they share a chord. Notice now that $\widehat{G}_C$ is a tree since G_C is connected and has one more region than it has chords, meaning $\widehat{G}_C$ must be connected and have one more vertex than it has edges.

Now we incorporate M into our construction. To do this, we interpret each chord of M as a new *edge* of $\widehat{G}_C$, connecting the vertices of the two regions it touches. In this way $\widehat{G}_C$ becomes a spanning tree of the resulting map, and the edges of M simply complete the cycles of this map. This transformation from a chord diagram with a chord partition to a map with a labelled spanning tree was injective because our actions were fully determined at every step.

For the second half of the proof we need to show the other direction of the correspondence. So, let Γ be a planar map with a marked spanning tree T. Say it has the associated vertex, edge, and face permutations ν, ε, and ϕ. The permutation ε admits a factorization into the product $\varepsilon_T \varepsilon_{\Gamma \setminus T}$, where

$$\varepsilon_T = \prod_{\substack{e=(e_1,e_2) \\ e \in E(T)}} (e_1\ e_2) \qquad \text{and} \qquad \varepsilon_{\Gamma \setminus T} = \prod_{\substack{e=(e_1,e_2) \\ e \in E(\Gamma \setminus T)}} (e_1\ e_2)$$

are products of transpositions. Since these two permutations have no common half-edges, they also commute.

Using the characterization of spanning trees in genus zero as one-face spanning submaps proven in Lemma 2.2.9, we can observe that the permutation $\nu\varepsilon_T$ is a cycle

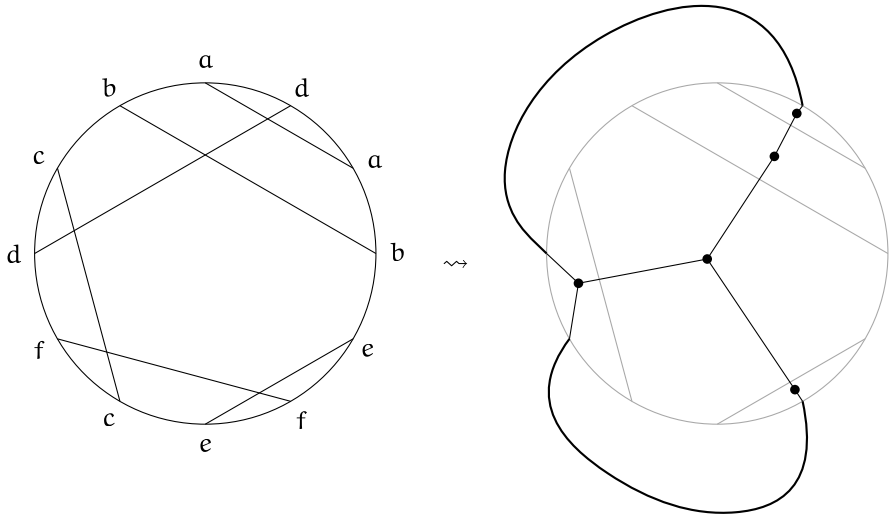

Figure 2.6: A graph obtained from a chord diagram. Notice that the interior edges on the right form a spanning tree of the resulting map, so this is determined entirely by the partition of the chord diagram.

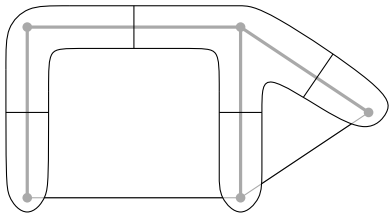

Figure 2.7: An example of the process of drawing a curve around a spanning tree to generate a chord diagram.

corresponding to a walk along the one face of the spanning tree T. This is our essential use of the genus in this proof.

We can draw a curve around the spanning tree sufficiently near to it that each edge not in the spanning tree is crossed exactly twice, and such that the order in which the half edges are touched corresponds with the order that half-edges not in T appear in the cyclic permutation $\nu\varepsilon_T$. This cyclic order, along with the connectivity information from $\varepsilon_{\Gamma\setminus T}$, specifies a chord diagram $C_{\Gamma\setminus T}$, and this is the same chord diagram one would get by deforming the curve around the spanning tree into a disc containing the edges of $\Gamma\setminus T$. The chord diagram C_T is similarly obtained from the cyclic order of the half edges from T in the cyclic permutation $\nu\varepsilon_T$. □

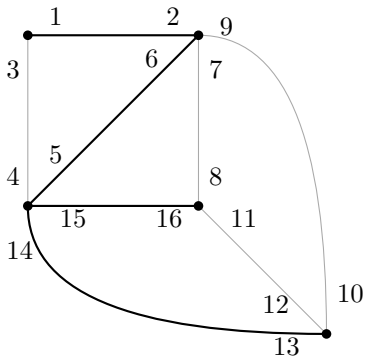

$\nu = (1\ 3)(2\ 9\ 7\ 6)(4\ 5\ 15\ 14)(8\ 11\ 16)(10\ 13\ 12)$

$\epsilon_T = (1\ 2)(5\ 6)(13\ 14)(15\ 16)$

$\nu\epsilon_T = (1\ 9\ 7\ 6\ 15\ 8\ 11\ 16\ 14\ 12\ 10\ 13\ 4\ 5\ 2\ 3)$

Figure 2.8: An example of the calculation of the cycle $\nu\epsilon_T$. The thick edges mark our choice of T. In this case C_T would be the chord diagram on the cycle $(1\ 6\ 16\ 14\ 13\ 5\ 2)$ with the four chords $1-2$, $5-6$, $13-14$, and $15-16$.

As a small remark on the construction laid out in proposition 2.2.10, notice that swapping M and $C \setminus M$ and then computing the resulting map gives the dual of the original map. Also, different partitions of the same chord diagram C can result in totally different maps. Since a chord diagram can admit partitions into pairs of non-crossing chord diagrams of completely different sizes, there can be no expectation that, say, the different partitions all amount to choices of spanning tree in one particular map, or that all the spanning trees in a particular map arise from choices of partition in one particular chord diagram.

2.2.4 Maps and Quadrangulations

This section will serve as a brief summary of the set of correspondences above. We began with maps with marked spanning trees, and we transformed them into quadrangulations with vertex- and face-colourings, found a canonical way to read Euler tours from those maps (remembering the vertex colouring along the way), realized those coloured tours as chord diagrams that partition into pairs of non-crossing subdiagrams, and transformed those diagrams back into maps in a way that recovered the original spanning tree.

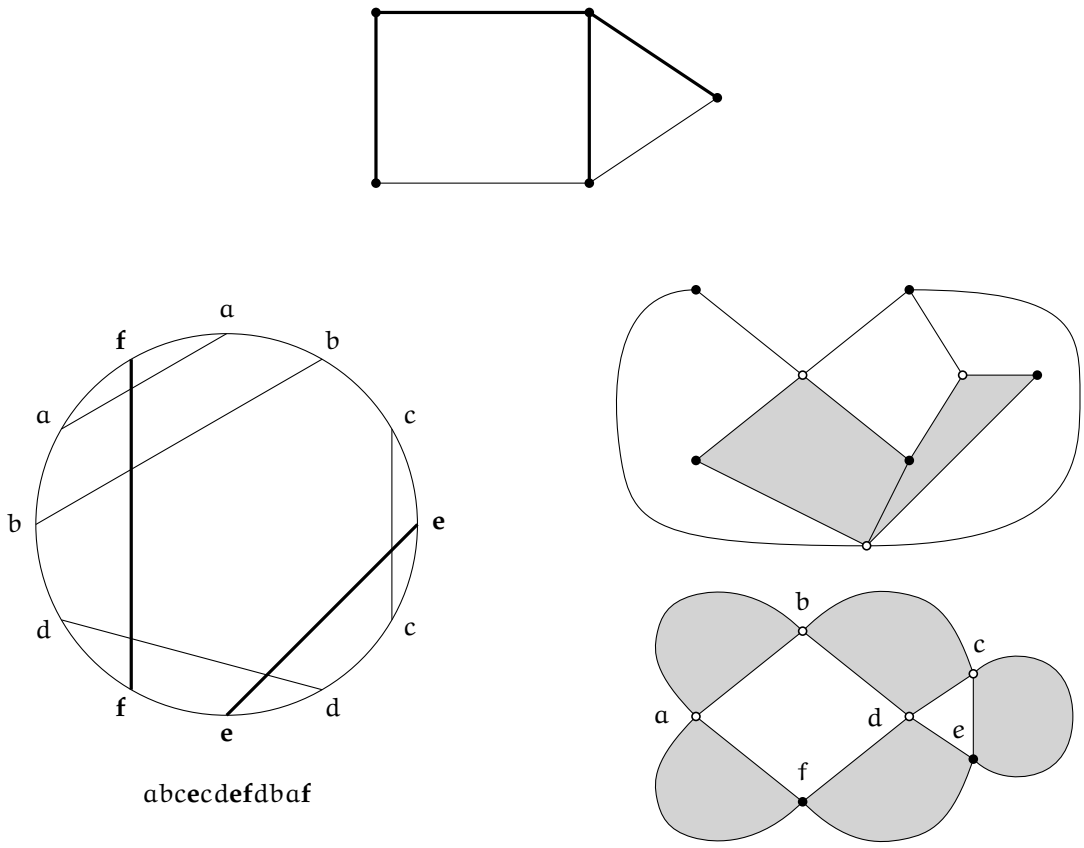

Figure 2.9: A full worked example of the cycle of correspondences in genus zero.

2.3 Positive Genus

Our goal now is to lift as many of the correspondences above from the planar case to surfaces of positive genus. The medial construction does not lift directly because quadrangulations in positive genus do not necessarily admit 2-face-colourings. A significant effort has been made to create robust analogies of the medial construction in positive genus [16], and there has been a successful, though difficult, extension to genus one [2]. However, the rest of the correspondences laid out in the last section will turn out to lift in a reasonable way. In effect, by constructing so many peripheral correspondences we will have built a path around this fundamental issue in positive genus.

As we saw in the proof of proposition 2.2.10, the essential fact about a spanning tree in the construction of a chord diagram from a map in genus zero was that it could be equivalently characterized in that genus as a one-face submap touching every vertex. In order to make the correspondence go through in other genera, we must take 'one-face submap touching every vertex' as the fundamental substructure to be labelled throughout. This is similar to the notion of 'quasitrees' appearing in, for example, [22]. The literature regarding these is very focused on a notion of 'partial duality' which may have a fruitful application here if explored in future work.

Lemma 2.3.1. Let M be a map of arbitrary genus g. For a submap T of M, the following are equivalent:

1. T is a spanning one-face submap of M,
2. T has one face and $|E(T)| = |V(M)| - 1 + 2g$,
3. T is spanning and $\nu\epsilon_T$ is a cyclic permutation of the half-edges in M.

Proof. 1 $\iff$ 2. Assume T is a spanning one-face submap of M. Then by Euler's formula applied to T, we have $|V(T)| - |E(T)| + 1 = 2 - 2g$. Since T is spanning, $|V(T)| = |V(M)|$, and we have the result by rearranging the last equation. On the other hand, assume T is spanning and $|E(T)| = |V(M)| - 1 + 2g$. Then by applying Euler's formula to T again, we learn that $|F(T)| = 1$ as desired.

1 $\iff$ 3. First we aim to compute ν in terms of ν_T. We can use the basic fact that if we have a cycle $(x_1\ x_2\ \dots\ x_k)$ and wish to insert an ordered list of terms $y_1, \dots, y_\ell$ all distinct from the x_i before some term x_{i_0}, we can write

$$(x_1\ x_2\ \dots\ x_{i_0-1}\ y_1\ \dots\ y_\ell\ x_{i_0}\ \dots\ x_k) = (x_{i_0}\ y_1\ \dots\ y_\ell)(x_1\ x_2\ \dots\ x_k).$$

As long as all the terms are distinct, we can insert as many lists as we like at as many positions as we like since all of these insertions commute, and we can perform insertions in permutations composed of multiple cycles since each insertion only effects one cycle. For a map M with submap T, we can thus write ν as a sequence of insertions on ν_T, say $\nu = \iota\nu_T$. With this in mind, assume T is a spanning one-face submap of M. Then $\nu\epsilon_T = \iota\nu_T\epsilon_T$ is simply the same series of insertions performed on the single cycle $\nu_T\epsilon_T$ and is therefore a cycle. In the other direction of implication, $\nu\epsilon_T = \iota\nu_T\epsilon_T$ is a cycle and so $\nu_T\epsilon_T$ is too, so T has one face as desired. □

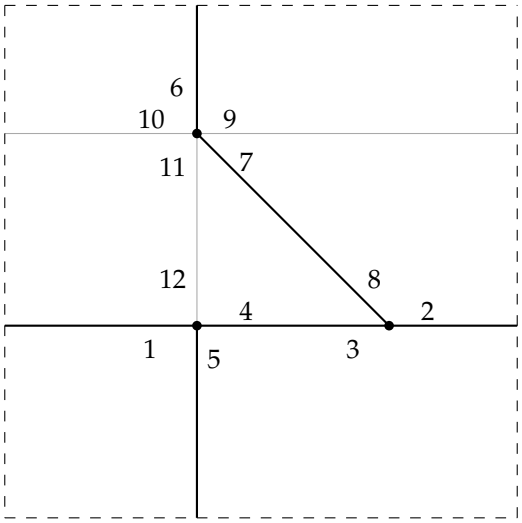

$\nu = (1\ 12\ 4\ 5)(2\ 3\ 8)(6\ 9\ 7\ 11\ 10)$

$\epsilon_T = (1\ 2)(3\ 4)(5\ 6)(7\ 8)$

$\nu\epsilon_T = (1\ 3\ 5\ 9\ 7\ 2\ 12\ 4\ 8\ 11\ 10\ 6)$

Figure 2.10: Example computation of the cycle $\nu\epsilon_T$ in a genus-1 map.

With the importance of one-face spanning submaps established, we are now prepared to lift the correspondence between maps and chord diagrams to higher genera. The specific subclasses of chord diagrams to be examined in each genus are novel. Given a surface of genus g, draw a closed curve bounding a disc, and consider the possible chord diagrams on the *outside* of that disc that can be drawn without crossing chords. Equivalently, consider the non-crossing chord diagrams that can be drawn on a disc with g handles glued onto it. We shall call such a chord diagram a *genus-g non-crossing chord diagram*. In particular, where in genus zero we had maps corresponding

to chord diagrams with a partition into a pair of chord diagrams with both being non-crossing, we lift in positive genus to pairs of chord diagrams with one being (genus-0) non-crossing, and one being genus-g non-crossing.

Genus-g non-crossing chord diagrams seem completely unstudied in the literature. While beyond the scope of this thesis, some obvious questions arise about the enumeration of such objects. If $F_g(x)$ is the generating series for genus-g non-crossing chord diagrams, we would have the relations $[x^n]F_g(x) \leqslant [x^n]F_{g'}(x)$ whenever $g \leqslant g'$. We also know that the coefficients of $F_0(x)$ are the Catalan numbers and $\lim_{g\to\infty} F_g(x)$ is the generating function for all chord diagrams. It would be valuable to know a closed form for $F_g(x)$ in terms of g and x. It would also be valuable to know whether the genus-g non-crossing chord diagrams admit a characterization in terms of forbidden subdiagrams for every g, and whether certain correspondences between non-crossing chord diagrams and connected chord diagrams studied by physicists lift to higher genera. Would such a correspondence then collapse to the identity in the $g \to \infty$ limit, or express some form of duality, or turn into some more complicated automorphism on the set of all chord diagrams on n chords? There are many variants of chord diagrams studied in the literature already, so it would also be valuable to know if there is a direct relationship with any of these.

The process for obtaining a map from such a chord diagram by placing the grey edges on the outside and performing something akin to dualizing *can* be lifted from the genus-zero case depicted in figure 2.6 if we add handles to our chord diagram as necessary, but this can quickly become difficult to do by hand. It is simpler to label the ends of the chords around the diagram as drawn in the standard way and then use that cycle to define the value of $\nu\epsilon_\top$. Since the chords and colouring encode both ϵ and $\epsilon_\top$ we can compute $\nu = (\nu\epsilon_\top)\epsilon_\top$, and we will have the information necessary to reconstruct the map by its permutations.

Now we are faced with the problem of translating a chord diagram of genus g into a new 4-regular map. We create the set of half edges for the new map by giving the letters of the cyclic string subscripts to distinguish between the pairs, and reading the vertex information from the cyclic order of the ends of chords around the diagram. Each chord x will have two sets of neighbours in the diagram, corresponding to the substrings ax_1b and cx_2d for some chords a, b, c, d, which may or may not be distinct. Call these the *neighbourhoods* of x in the cyclic string. To construct the permutations for our new map, we begin by creating symbols $\overrightarrow{ax_1}, \overleftarrow{bx_1}, \overrightarrow{cx_2}, \overleftarrow{dx_2}$ with x on the right and arrows corresponding to the incidence direction in the cyclic word. To construct the permutation ν', we include one of the two cycles $(\overrightarrow{ax_1}\ \overleftarrow{bx_1}\ \overrightarrow{cx_2}\ \overleftarrow{dx_2})$ or $(\overrightarrow{ax_1}\ \overleftarrow{bx_1}\ \overrightarrow{cx_2}\ \overleftarrow{dx_2})^{-1}$

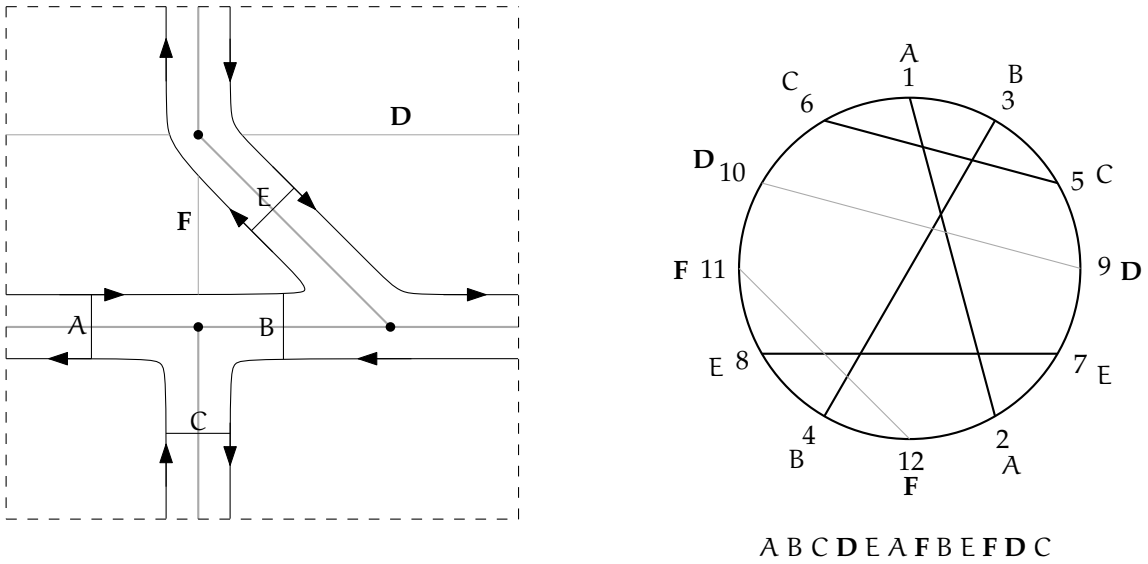

Figure 2.11: Interpretation of the cycle $\nu\epsilon_T$ as a chord diagram using edges from ϵ, and cyclic string corresponding to cyclic incidence of the chords around the circle. Equivalently the chord diagram can be constructed by walking along the face of T to create a closed curve bounding a disc on one side and drawing chords as depicted here.

from every x, depending on the colour of x in the chord diagram. To construct ϵ' we include the edge $(\overrightarrow{xy}\ \overleftarrow{yx})$ for every pair of consecutive characters xy in the cyclic string.

While this is enough information to construct the 4-regular map, we can actually read the faces off of the chord diagram by walking clockwise along the outside, walking along the dark chords, and walking past the light chords. Likewise, we can read the faces of the original map by walking along the light chords and across the dark ones.

2.4 The Coefficient-Level Formula

With all the structure of the bijections finally elucidated, we turn to the task of 'genus-shifting', i.e., the question of obtaining the lower-genus maps corresponding to a quadrangulation in the coefficient-level formula, or equivalently raising a map's genus to obtain a particular quadrangulation of higher genus. Once again, the coefficient-level

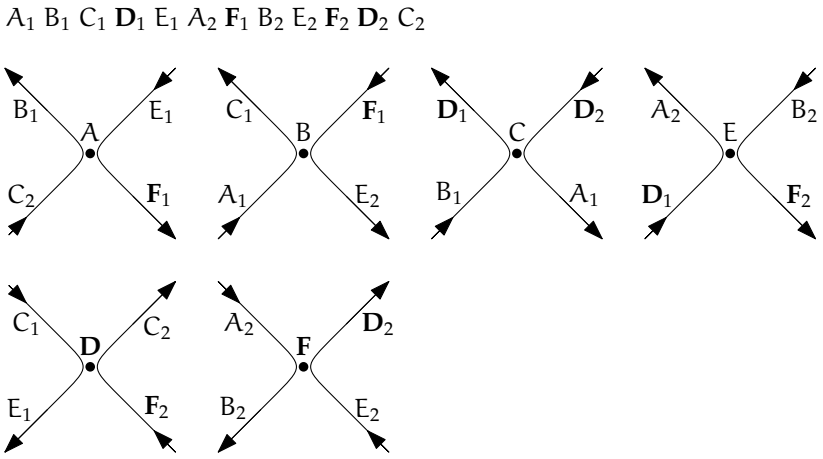

Figure 2.12: Reading the vertex information for a 4-regular map from the cyclic string. Since we know how the half-edges fit together unambiguously and we know the cyclic order around every vertex, we can compute the faces and thus the structure of the entire map in a unique way.

formula is

$$q(g, 2e) = \sum_{\gamma=0}^{g} \sum_{f=1}^{\infty} 2^{2\gamma} \binom{f}{2g-2\gamma} a(\gamma, f, e).$$

Proposition 2.4.1. Let $e_\gamma^T(v) = v - 1 + 2\gamma$ be the number of edges in a spanning one-face submap of a genus-γ map with v vertices. Then in the formula above,

$$\binom{f}{2g-2\gamma} = \binom{e+1-e_\gamma^T(v)}{2g-2\gamma} = \binom{e+1-e_\gamma^T(v)}{e+1-e_g^T(v)}.$$

Proof. By Euler's formula,

$$\begin{aligned} f &= 2 - 2\gamma - v + e \\ &= 1 + e - e_\gamma^T(v) \end{aligned}$$

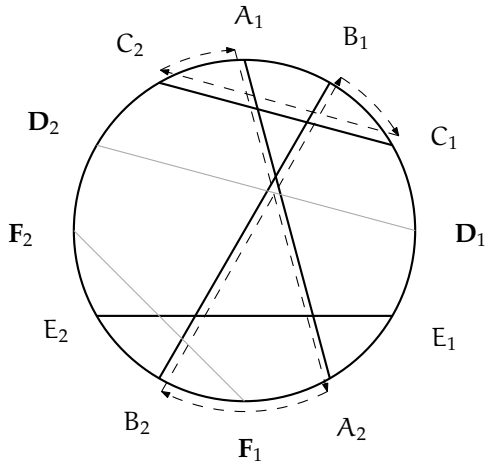

Figure 2.13: Walking in the chord diagram to read a face of the 4-regular map.

which gives $\binom{f}{2g-2\gamma} = \binom{e+1-e_\gamma^T(\nu)}{2g-2\gamma}$. For the other equality,

$$\begin{aligned}\binom{e+1-e_\gamma^T(\nu)}{2g-2\gamma} &= \binom{e+1-e_\gamma^T(\nu)}{2-2\gamma-\nu+e-2g+2\gamma} \qquad \text{(since } \tbinom{a}{b} = \tbinom{a}{a-b}\text{)}\\ &= \binom{e+1-e_\gamma^T(\nu)}{2-\nu+e-2g}\\ &= \binom{e+1-e_\gamma^T(\nu)}{e+1-e_g^T(\nu)}. \qquad \square\end{aligned}$$

So, take an arbitrary map G. We can try to raise its genus in a way that seems to be combinatorially evocative of the formula

$$q(g,2e) = \sum_{\gamma=0}^{g}\sum_{\nu=1}^{\infty} 2^{2\gamma}\binom{e+1-e_\gamma^T(\nu)}{2g-2\gamma}a(\gamma,f,e)$$

by the following process.

1. Add a self-loop with corresponding transposition $t = (h+1\ h+2)$ (here h was the number of half-edges in the original map) directly before the root half-edge, and remember that this edge was special. The addition of t will modify ν and ϵ by giving permutations $\nu^+ = (1\ h+1\ h+2)\nu$, $\epsilon^+ = \epsilon t$, and $\epsilon_T^+ = \epsilon_T$. Notice that $\nu^+\epsilon_T^+ = (1\ h+1\ h+2)\nu\epsilon_T$, which is still a cycle if $\nu\epsilon_T$ was.

2. Choose edges $e_1, \ldots, e_{2g-2\gamma}$ not in the spanning one-face submap, with corresponding transpositions $t_1, \ldots, t_{2g-2\gamma}$.

3. Set $\epsilon' = \epsilon^+$, $\epsilon'_T = \epsilon^+_T t_1 \cdots t_{2g-2\gamma}$ and $\nu' = \nu^+ t_1 \cdots t_{2g-2\gamma}$. This creates a new map G' with $\nu'\epsilon'_T = \nu^+\epsilon^+_T$, which is once again a full cycle as long as $\nu\epsilon_T$ was.

We have the following weak result on the application of this strategy to genus-raising.

Proposition 2.4.2. If the edges e_i corresponding to the transpositions t_i all have the property that both ends hit the same vertex and both sides touch the same face, then the map G' has genus g.

Proof. We shall induct on $g - \gamma$. In the case $g - \gamma = 0$, we get $G' = G^+$, which is just G with an extra self-loop on the root vertex immediately before the root half-edge. Now say $g-\gamma > 0$, and say we have chosen $\epsilon'_T = \epsilon^+_T t_1 \cdots t_{2g-2\gamma}$ and $\nu' = \nu^+ t_1 \cdots t_{2g-2\gamma}$. Then we know that the map G'' given by $\epsilon'' = \epsilon^+$ and $\nu'' = \nu^+ t_1 \cdots t_{2g-2\gamma-2}$ has genus $g-1$ by induction, so we may dispense with the extra terms, replace G with G'', and assume without loss of generality that $g - \gamma = 1$, and that we are only examining transpositions t_1 and t_2.

We must determine how many vertices and faces the map G' has to compute its genus. This depends on t_1 and t_2. If the edge corresponding to t_1 has both ends on the same vertex in G^+ then multiplication by t_1 will increment the number of cycles in ν^+, and if not then it will decrement the number of cycles in ν^+. Similarly t_2 will do the same to $\nu^+ t_1$. For ϕ', observe that

$$\begin{aligned}\phi' &= \nu'\epsilon' \\ &= \nu^+ t_1 t_2 \epsilon^+ \\ &= \nu^+ \epsilon^+ t_1 t_2 \\ &= \phi^+ t_1 t_2.\end{aligned}$$

So if the edge e_1 corresponding to t_1 has the same face on both sides in G^+ then multiplication by t_1 will increment the number of cycles in ϕ^+ (and if not then multiplication by t_1 will *decrement* the number of cycles in ϕ^+), and similar for t_2 and $\phi^+ t_1$. Now, if e_1 has both ends on the same vertex in G^+ then an analogous argument shows that $\nu t_1 t_2$ will have two extra cycles. If both of these phenomena occur then applying Euler's formula shows that the genus has indeed increased as desired. □

Chapter 3

Cycle Decompositions of 4-Regular Graphs

3.1 Background

Introduced in a series of papers published in 2014 and 2015 [4–9], the CHY formalism is a way of rewriting the Feynman integrals in various quantum field theories as integrals over the moduli space $\mathcal{M}_{0,n}$ when the integral concerns the interaction of n particles. Let $\alpha : i \mapsto \alpha_i$ be a cyclic permutation of $\{1, \ldots, n\}$. Of importance in the CHY integral formulation are the *Parke-Taylor factors*

$$C_n[\alpha] = \frac{1}{\sigma_{\alpha_1\alpha_2}\sigma_{\alpha_2\alpha_3}\cdots\sigma_{\alpha_{n-1}\alpha_n}\sigma_{\alpha_n\alpha_1}} \qquad \text{where} \qquad \sigma_{ij} = \sigma_i - \sigma_j.$$

The σ_i are variables to be integrated over in the near future. Terms of this form originally appeared in a formula for computing the so-called maximally helicity violating amplitudes in Yang-Mills theory [23]. Pairs of Parke-Taylor factors are combined in the expression $m_n[\alpha|\beta]$ which is a particular integral over all the σ_i involving the product $C_n[\alpha]C_n[\beta]$. The following set-up lets us compute $m_n[\alpha|\beta]$ combinatorially.

Definition 3.1.1. If a tree with leaves labelled $1, \ldots, n$ can be drawn in the plane with leaves appearing in the cyclic order $\alpha_1, \ldots, \alpha_n$, we call it *$\alpha$-ordered*. Define $\mathcal{T}[\alpha]$ to be the set of trees with n leaves and internal vertices of degree 3 which are α-ordered.

Theorem 3.1.2 ([24]). Up to a sign,

$$m_n[\alpha|\beta] = 2^{n-3} \sum_{g \in \mathcal{T}[\alpha] \cap \mathcal{T}[\beta]} \prod_{e \in E(g)} \frac{1}{s_e}$$

where s_e is the square of the momentum along the edge e, considering g as a Feynman diagram.

An important consequence of theorem 3.1.2 is that $\mathcal{T}[\alpha]$ and $\mathcal{T}[\beta]$ are disjoint if and only if $m_n[\alpha|\beta] = 0$, suggesting a notion of orthogonality for cycles.

Now we intend to generalize $m_n[\alpha|\beta]$ to arbitrary permutations. If we take a permutation π with many cycles, we can still write down a Parke-Taylor factor for π, as the product of the Parke-Taylor factors for each of its cycles. Moreover, if π has no fixed points, if we take a cycle α and try to compute $m_n[\alpha|\pi]$ it is often the case that by rearranging the $\frac{1}{\sigma_{\pi_i,\pi_{i+1}}}$ and the $\frac{1}{\sigma_{\alpha_j,\alpha_{j+1}}}$ we can say $m_n[\alpha|\pi] = m_n[\alpha'|\beta']$ for two cycles α' and β'. We can equivalently view the fixed-point-free permutations π as 2-regular graphs with no self-loops. With this in mind we can even write $m_n[G|H]$ for 2-regular graphs G and H.

As a real vector space, $\mathcal{M}_{0,n}$ is known to be $(n-3)!$-dimensional. If it can be shown there are $(n-3)!$ pairwise orthogonal 2-regular graphs, we will have created a potentially useful structure on top of $\mathcal{M}_{0,n}$. This problem splits into two steps: if we can show first that any 2-regular graph G has enough cycles C with the property that $m_n[G|C] = m_n[C'|C'']$ for two cycles C' and C'', and second that enough of these C are pairwise orthogonal, then we will be done. The contribution of this chapter is to solve the first half of this problem.

From a physical point of view, when α and β are cycles the integral $m_n[\alpha|\beta]$ is a sum of Feynman diagrams which are trees, and when they are not then the Feynman diagrams can be arbitrary graphs. If it can be shown that for arbitrary α and β, $m_n[\alpha|\beta]$ decomposes into a finite linear combination of tree-level integrals, then we will have a reasonable means of computing arbitrary Feynman integrals in the applicable quantum field theories.

3.2 Bounding the number of compatible cycles in general

These results first appeared in the paper [10], which was co-authored by the author of this thesis.

Definition 3.2.1. The *edge-disjoint union* of two graphs G and H on the same vertex set V, denoted simply $G \cup H$, is the graph whose vertex set is V and whose edge set is $E(G) \sqcup E(H)$. The square union symbol here means that these sets are forcibly disjoint; any shared edges get duplicated in the resulting graph.

To begin, we are given a 2-regular (multi)graph G, or equivalently a disjoint union of cycles, on the vertices $\{1, \ldots, n\}$. We are interested in finding cycles C on $\{1, \ldots, n\}$ such that $G \cup C$ admits a new decomposition as $C_1 \cup C_2$, with both C_1 and C_2 being cycles. In particular, we want to count how many C induce such a decomposition for a fixed G, or at least show that this number is relatively large. This motivates the following definition.

Definition 3.2.2. For a 2-regular graph G, a cycle C is said to be *compatible to* G if $G \cup C$ admits a decomposition into a union $C_1 \cup C_2$ of two cycles.

Theorem 3.2.3. When G consists of only even cycles, there are more than $(n-3)!$ compatible cycles to G. In fact, there are at least $(n-2)!/2$ such cycles.

We can do this with the help of two lemmas, as follows. First, since G is bipartite, we decompose G as $G = A \cup B$ with A and B perfect matchings on G, so that G consists of AB-alternating cycles.

Lemma 3.2.4. With G as above, there exist at least $(n-2)!!$ choices for a perfect matching P on the vertices of G such that $P \cup A$ is a cycle.

Proof. Pick a vertex $v \in G$. Let its neighbour in A be a and its neighbour in B be b. Starting from v, draw a P-edge from v to some vertex p which is distinct from a and v. There are then $n-2$ choices for the edge vp. Now continue as follows: let v' be the neighbour of p in A, and choose one of the $n-4$ remaining vertices to join it with in P. Continuing by induction there are $(n-2)!!$ choices for P. □

Lemma 3.2.5. With G, A, B, and a choice of P as before, there are at least $(n-3)!!$ choices for a perfect matching Q with the property that both $Q \cup B$ and $P \cup Q$ are cycles.

Proof. This proof is the main part of the whole argument for the general result. We proceed by induction. In the base case $n = 4$ and the result follows by checking several diagrams: either G is a 4-cycle or it is a pair of 2-cycles. In either case, we can simply draw enough Q no matter the choice of P, as in the following figure.

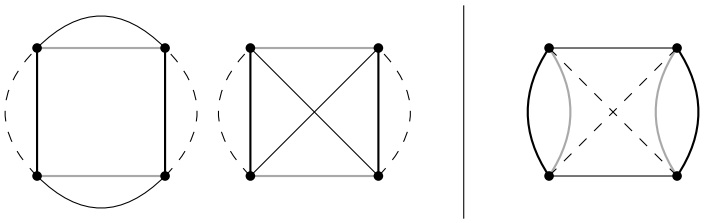

Figure 3.1: The base case for the lemma. Thick black edges are A, thick grey edges are B, thin black edges are P, and thin dashed edges are Q.

For the induction, first pick a vertex v. Label its A-neighbour a, its B-neighbour b, and its P neighbour p. Pick a vertex q not in $\{v, b, p\}$ and draw a Q-edge vq. Given such a choice of q, label its A-neighbour α, its B-neighbour β, and its P-neighbour π. From here, we create a new graph G' as follows: set $V(G') := V(G) \setminus \{v, q\}$, and let $E(G')$ be the set of all those edges in G which avoid v and q, along with the edges $a\alpha$, $b\beta$, and $p\pi$. The graph G' inherits a natural decomposition into three matchings from G. These

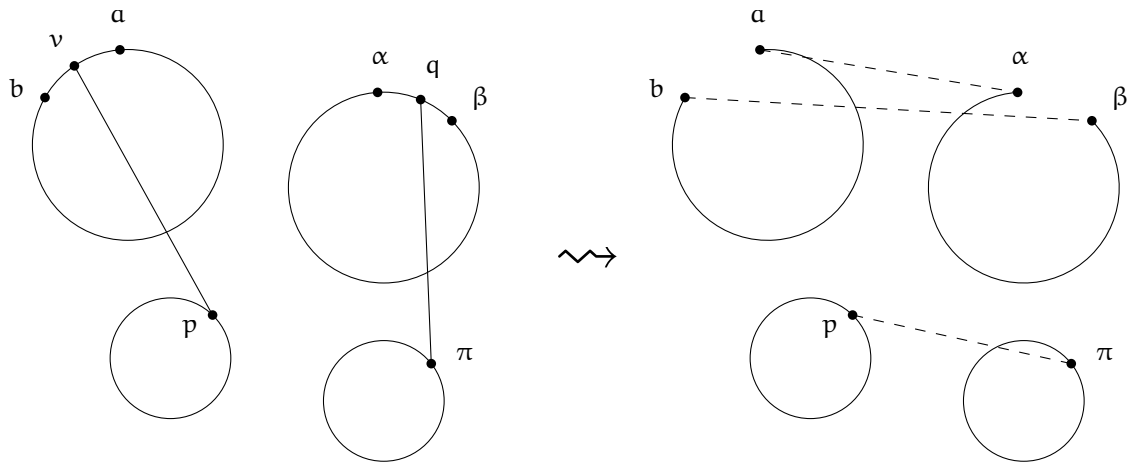

Figure 3.2: A demonstration of the construction of G' from G.

are $A' = (A \cap G') \cup \{a\alpha\}$, $B' = (B \cap G') \cup \{b\beta\}$, and $P' = (P \cap G') \cup \{p\pi\}$. It should be noted that these are indeed matchings, since none of $a, b, p, \alpha, \beta, \pi$ are saturated in the restrictions of their respective matchings to G'. Certainly all of these matchings are also perfect. Now, G' and the three matchings satisfy the induction hypothesis, and so give rise to $(n-2-3)!!$ choices of Q' with the property that both $C'_B := Q' \cup B'$ and $C'_P := P' \cup Q'$ are cycles.

From here the goal is to lift Q' up to the perfect matching $Q := Q' \cup \{vq\}$ on G and

show that Q satisfies the lemma. To this end, note that $C'_B \setminus \{b\beta\}$ and $C'_P \setminus \{p\pi\}$ induce paths S_B and S_P on G which hit all of the vertices except ν and q. Notice now that $S_B \cup \{b\nu, \nu q, q\beta\}$ is a cycle consisting of all of the edges of B and Q, and $S_P \cup \{p\nu, \nu q, q\pi\}$ is a cycle consisting of all the edges of P and Q. This means Q satisfies the lemma.

Now, there were at least $n-3$ choices for the edge νq and at least $(n-5)!!$ choices for the matching Q'. If there is no repetition here, we will have at least $(n-3)!!$ choices for Q and the claim will be proven. To see that there is indeed no repetitition, note that two different choices of q cannot lead to the same cycle, and given the same choice of q, the paths S_B and S_P will depend only on the (already distinct) choices of Q'. This completes the proof. □

Proof of Theorem 3.2.3. We simply multiply the numbers in the results of the last two lemmas and divide by two since the matchings P and Q are indistinguishable. The result is

$$\frac{(n-2)!!(n-3)!!}{2} = \frac{(n-2)}{2}(n-3)! \geqslant (n-3)!$$

as desired. □

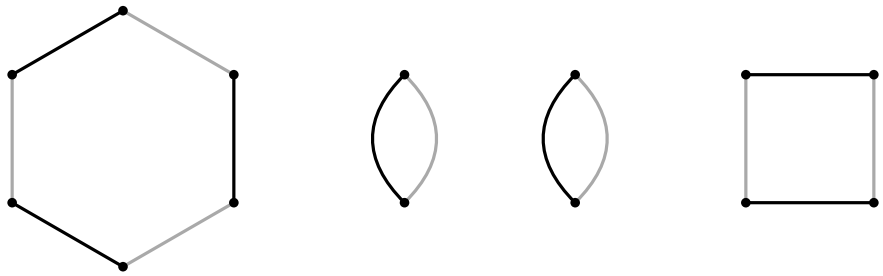

Figure 3.3: An example graph G with all even cycles decomposed as $A \cup B$, with the black edges being A and the grey edges being B.

To illustrate how this theorem can be used algorithmically to construct compatible cycles, consider the example in figure 3.3. By the first lemma we can construct the perfect matching P by beginning at a vertex, say the upper of the two leftmost vertices in the figure, following A, in this case to the top vertex, and then choosing any vertex other than the two already mentioned to join to the top vertex making an edge for P. Suppose we choose the lower of the two vertices to the right in the same cycle of G. Then we follow A again and pick any vertex not already seen to add a new edge to P and so on. Continuing in this way one possible P we could obtain is as illustrated in Figure 3.4.

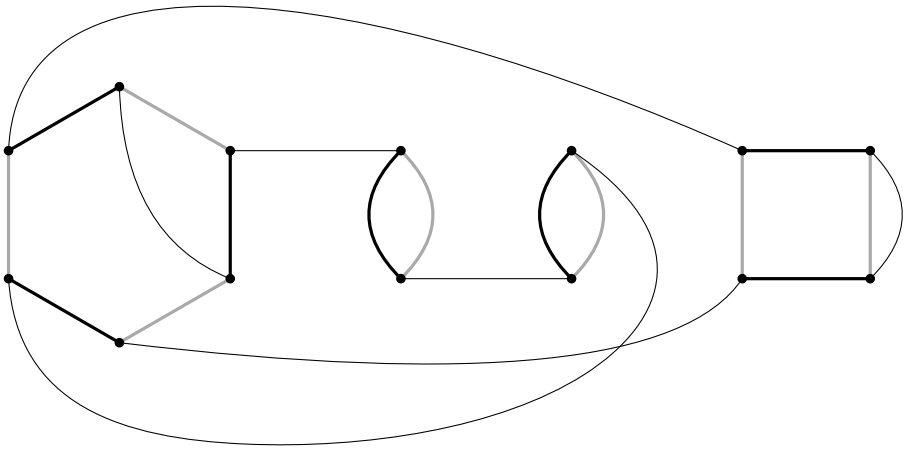

Figure 3.4: The example graph G along with a perfect matching P given by the thin black edges, so that $P \cup A$ is a cycle.

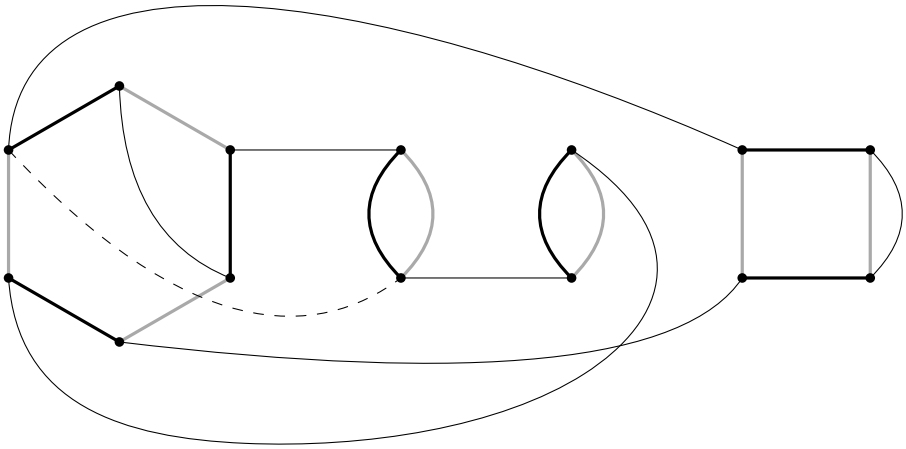

Figure 3.5: G and P along with a first edge for the construction of Q, drawn dashed here.

Next we follow the second lemma. Beginning again at the upper of the two leftmost vertices, we pick any vertex other than this vertex's neighbours in B and P to make an edge for Q. In this case, say we pick the lower vertex of the leftmost 2-cycle. This is illustrated in figure 3.5.

From this choice of edge the second lemma tells us to construct G' (along with P') as illustrated in figure 3.6.

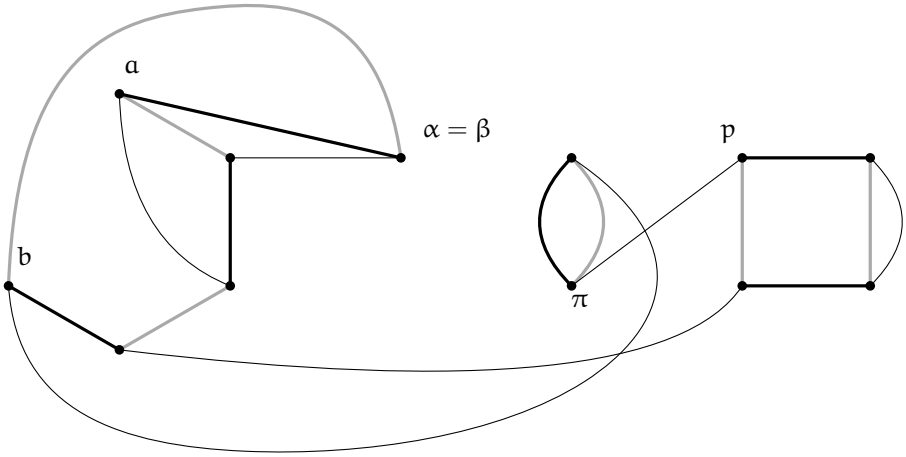

Figure 3.6: The graph $G' = A' \cup B'$ with P'.

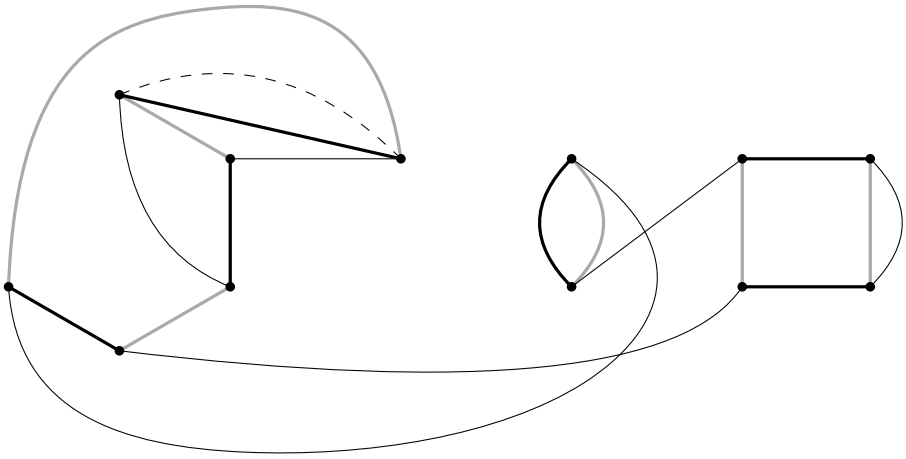

Figure 3.7: The graph $G' = A' \cup B'$ with P', along with a first choice of edge for Q'

The process now continues. Progressing one more step explicitly, choose the first edge of Q' as shown in figure 3.7. This results in the graph G'' as illustrated in figure 3.8. Continuing this process we can construct Q''. One possibility for Q'' is shown in figure 3.9.

Bringing Q'' up to Q' on G' we obtain the situation illustrated in figure 3.10, and bringing Q' up to Q on G we obtain our compatible cycle $P \cup Q$ as illustrated in figure 3.11. Observe that in this last figure, $A \cup P$, $B \cup Q$, and $P \cup Q$ are all cycles as expected.

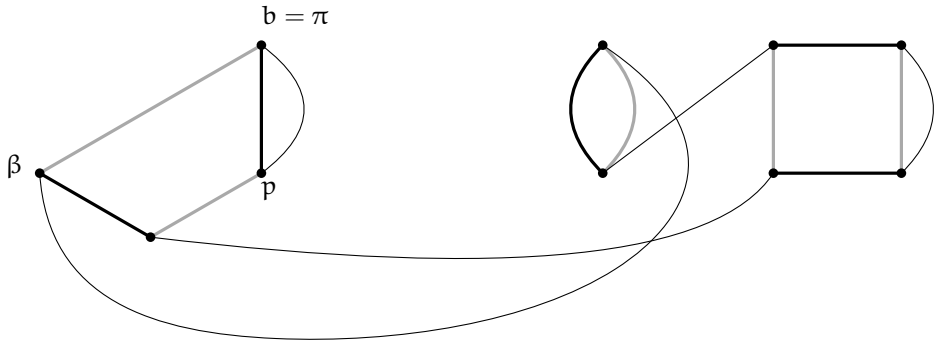

Figure 3.8: The graph $G'' = A'' \cup B''$ with P''.

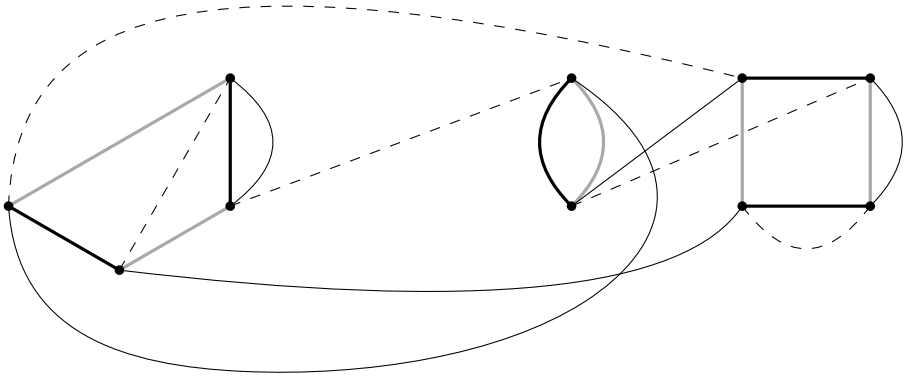

Figure 3.9: The graph $G'' = A'' \cup B''$ with both P'' and Q''.

As this worked example shows, the theorem in fact gives an algorithm to generate $(n-2)!/2$ compatible cycles for any 2-regular graph G with all even cycles.

Theorem 3.2.6. For an arbitrary 2-regular graph G, there are more than $(n-3)!$ compatible cycles to G. In particular, there are at least $(n-2)!/4$ such cycles.

Proof. To start, let $O_1, \ldots, O_k$ be the odd cycles of G. Pick a vertex v_i from each O_i. Now we will 'bandage' these cycles at the v_i in the sense that they will be treated just as a point along the 'single edge' between their neighbours. From this perspective we have reduced the graph G to a graph G' with only even cycles on $n-k$ vertices. Applying the previous theorem, there are $(n-k-2)!/2$ choices for C on the bandaged graph G'.

Now we must extend C to the full graph. Assume we partition G' into a pair of perfect matchings $A \cup B$ as before, and assume our compatible cycle decomposes into a pair of perfect matchings $P \cup Q$ as before. We would like to do this by, for each v_i

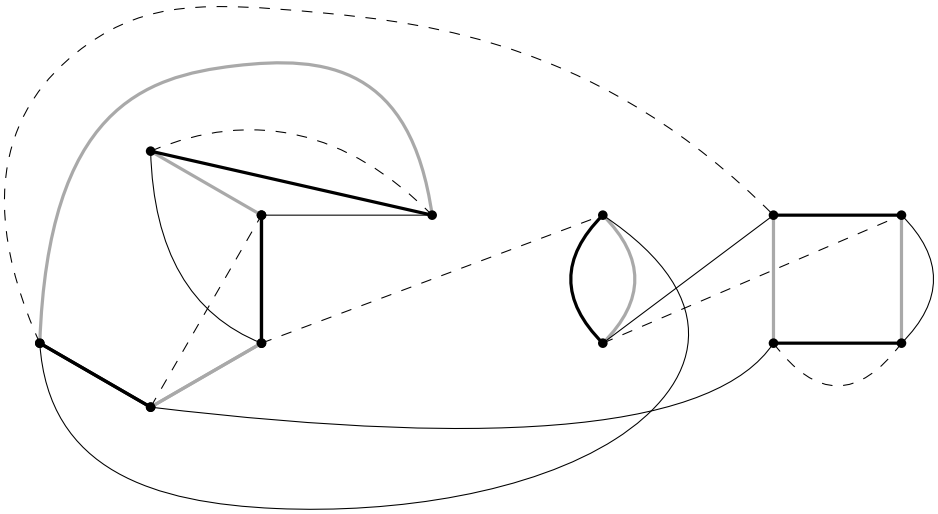

Figure 3.10: The graph $G' = A' \cup B'$ with both P' and Q' inherited from G''.

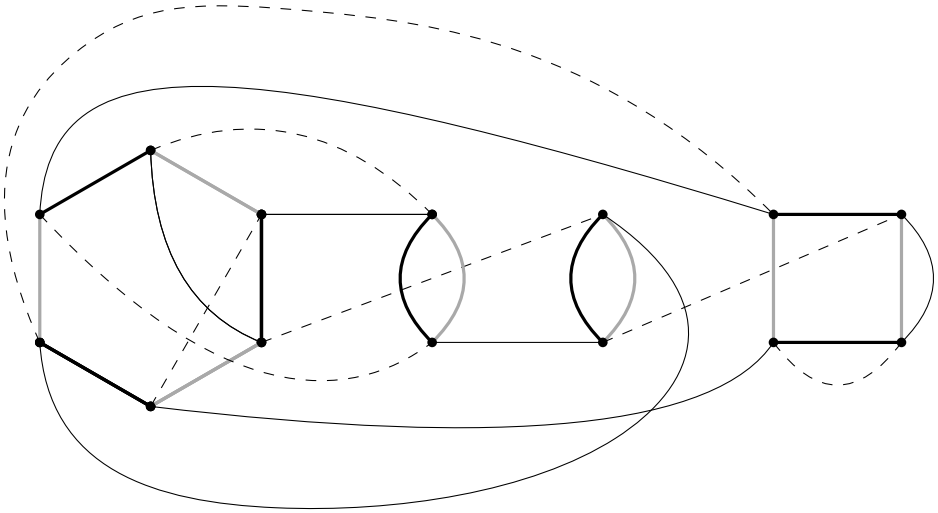

Figure 3.11: The graph $G = A \cup B$ with P and Q. The thick black edges are A, the thick grey edges are B, the thin black edges are P and the thin dashed edges are Q.

in turn, picking an edge ww' of C and replacing it with wv_iw'. As we reroute we increase the number of edges by one each time, and so there would be $(n-k)(n-k+1)\cdots(n-1)$ choices of how to extend C. However, not every choice of ww' preserves the compatibility of C. Indeed, as in figure 3.12, if v_i sits along an edge in A and the

edge ww' is in P, then $P \cup A$ will not remain a cycle because v_i will have degree 4 in $P \cup A$. The same would be true for $B \cup Q$ if v_i were along a bandaged edge in B and ww' were in Q.

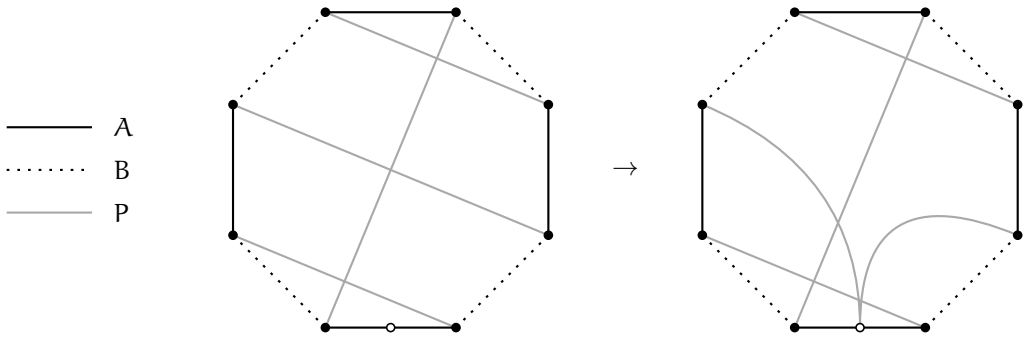

Figure 3.12: An example of a bandaged graph consisting of one odd cycle. The matching Q is not drawn for clarity, and the bandaged vertex is marked in white. If we extend our choices of A, B, and P to the original graph by picking the edge ww' from P, $A \cup P$ will not be a cycle.

So, instead of picking an arbitrary edge ww', we must pick edges from the correct choice of P or Q. As we reroute edges and unbandage vertices, A, B, P and Q will not remain matchings, but this is not a problem, since we only care about $A \cup B$, $A \cup P$, and $A \cup Q$ being cycles, and they still will be. So we begin with $(n-k)/2$ choices, and at every step we gain one additional choice in either P or Q. So, if there are k_A bandaged vertices in A and k_B bandaged vertices in B, then we will have $k = k_A + k_B$ and we will get a total of

$$\left(\frac{n-k}{2}\right)\left(\frac{n-k}{2}+1\right)\cdots\left(\frac{n-k}{2}+k_A-1\right) \cdot \left(\frac{n-k}{2}\right)\left(\frac{n-k}{2}+1\right)\cdots\left(\frac{n-k}{2}+k_B-1\right)$$

choices in total. The smallest this number can be is when $k_A = k_B = k/2$, causing the expression to simplify, giving

$$\begin{aligned}\frac{\left(\frac{n}{2}-1\right)!^2}{\left(\frac{n-k}{2}-1\right)!^2} &= \frac{1}{2^{2k/2}}\frac{(n-2)!!^2}{(n-k-2)!!^2} \\ &\geqslant \frac{1}{2^k}\frac{(n-2)!}{(n-k-2)!}\end{aligned}$$

choices.

Keeping the v_i fixed, note that in the initial choice of decomposition of G' into A and B, each v_i is either in A or in B. Let us fix a choice of A and B for G' with v_1 along an A-edge. Suppose we have a compatible cycle C for G constructed as above based on this choice of A and B. Then the edges of C alternate between P and Q except at the v_i where two edges in the same set occur consecutively. Since we know v_1 is along an A-edge in G' , the construction above gives that v_1 is between two Q-edges in C. Following the alternation of edges around C, starting with the Q-edges around v_1 we can determine for each v_i whether it is surrounded by P-edges or Q-edges. If a v_i is surrounded by P-edges in C then it lies along a B-edge in G' and if v_i is surrounded by Q edges in C then it lies along an A-edge in G'.

This means that knowing a compatible cycle C constructed as described above and knowing that v_1 is along an A-edge in G' is enough to determine which v_i lie along an A-edge and which lie along a B-edge in G'. However, this choice comes from our initial choice of decomposition of G' into A and B. Consequently, different choices of how the v_i are assigned to edges in A and B must give different compatible cycles C. Since the argument required us to fix v_1 along an A-edge, it remains to choose which of A or B for the v_i for $2 \leqslant i \leqslant k$. That is, there remain $k-1$ binary choices. Together with the construction given above for C, this means that we obtain a total of at least

$$2^{k-1} \cdot \frac{1}{2^k} \frac{(n-2)!}{(n-k-2)!} \cdot \frac{(n-k-2)!}{2} = \frac{1}{4}(n-2)!$$

choices for a compatible cycle C. When $n \geqslant 6$ this proves the theorem. For $n < 6$ we refer the reader to the explicit computation for small n in [3]. □

3.3 Breakpoint Graphs

There is a surprising relationship between the enumeration of compatible cycles and the study of genomic rearrangements in bioinformatics. In [15], the authors give the following series of definitions reformulating a concept originally appearing in [1].

Definition 3.3.1. Given vertices $\{0, 1, \ldots, 2m, 2m+1\}$, define the perfect matching $\delta_G = \{\{2i, 2i+1\} : 0 \leqslant i \leqslant m\}$. A *configuration* is a union $\delta_B \cup \delta_G$ with δ_B being another perfect matching.

Definition 3.3.2. Let $\overline{\delta}_G = \{\{2i-1, 2i\} : 1 \leqslant i \leqslant m\} \cup \{\{2m+1, 0\}\}$. Given a configuration $\delta_G \cup \delta_B$, define the *complement* of $\delta_G \cup \delta_B$ to be $\overline{\delta}_G \cup \delta_B$.

Definition 3.3.3. A *signed permutation* π is a permutation of the set $\{-n, -n+1, \ldots, -2, -1, 1, 2, \ldots, n-1, n\}$ with the property that $\pi(-i) = -\pi(i)$. The set of signed permutations on $\{-n, -n+1, \ldots, -2, -1, 1, 2, \ldots, n-1, n\}$ forms a group, which is called the *hyperoctahedral group*, denoted $S_n^{\pm}$.

Definition 3.3.4. Given a signed permutation $\pi : i \mapsto \pm\pi_i$ in $S_n^{\pm}$, transform it into an unsigned permutation $\pi' \in S_{2n}$ by mapping positive π_i to the sequence $(2\pi_i - 1, 2\pi_i)$ and negative π_i onto the sequence $(2\pi_i, 2\pi_i - 1)$. Define a matching $\delta_B(\pi) := \{\{\pi'_{2i}, \pi'_{2i+1}\} : 0 \leqslant i \leqslant n\}$. The *breakpoint graph* of π is the graph $BG(\pi) := \delta_B(\pi) \cup \delta_G$.

Definition 3.3.5. The *signed Hultman number* $S_H^{\pm}(m, k)$ is the number of signed permutations on m elements whose breakpoint graph has exactly k disjoint cycles.

The following lemma is proven in [15], and we can use it to relate signed Hultman numbers to the enumeration of compatible cycles.

Lemma 3.3.6 (Grusea-Labarre)**.** A configuration $\delta_B \cup \delta_G$ is a breakpoint graph if and only if the complement $\delta_B \cup \overline{\delta}_G$ is a cycle.

Using this lemma, we can improve our bounds from the last section to an exact count of the compatible cycles in one particular case.

Theorem 3.3.7. The number of compatible cycles to a graph G consisting of n vertices with $n/2$-many 2-cycles is exactly

$$\frac{1}{2}(n-2)!!S_H^{\pm}(n/2-1, 1).$$

Proof. First, we claim that the one-cycle breakpoint graphs on $n = 2m+2$ vertices are exactly the compatible cycles to a graph consisting of $n/2$-many 2-cycles. If C is a breakpoint graph with one cycle on $2m+2$ vertices, then by lemma 3.3.6, the cycle C can be written as $\delta_B \cup \delta_G$ with $\delta_B \cup \overline{\delta}_G$ also a cycle, and so C is a compatible cycle for $G = \overline{\delta}_G \cup \overline{\delta}_G$, the graph consisting of $(2m+2)/2$ disjoint pairs of double edges. The other direction of the claim is clear. It is also shown in [15] that the number of breakpoint graphs on $m+1$ cycles with $2m+2$ vertices is $S_H^{\pm}(m, 1) = S_H^{\pm}(\frac{n}{2} - 1, 1)$.

Finally, we need to consider how many different labellings of G would result in different families of breakpoint graphs. This is asking, given $\overline{\delta}_G$, how many different δ_G could it correspond to? This question is answered by lemma 3.2.4: there are $(n-2)!!$ such δ_G. Once again we need to divide by 2 since either of the two matchings could have been δ_G. Multiplying everything together gives the result. □

This formula was conjectured by Cachazo and Gomez in [3], where it is also shown that asymptotically

$$\frac{1}{2}(n-2)!!S_H^{\pm}(n/2-1,1) \sim \frac{\pi}{4}n(n-3)!.$$

This means that in the case of a 2-regular graph where all of the cycles have size 2, comparing this asymptotic with the lower bound of $(n-2)!/2$ in theorem 3.2.3 finds a ratio tending to $\pi/2$ as $n \to \infty$.

Chapter 4

Conclusions

In chapter 2 we began with genus-zero maps and demonstrated a cycle of bijections from quadrangulations with face colourings, to Euler tours of four-regular graphs, to chord diagrams partitioned into pairs of non-crossing subdiagrams, to maps with a marked spanning tree. We then lifted this correspondence to higher genera, where the role of the spanning tree from before was played by a spanning one-face submap. The partitioned chord diagrams changed as well: in positive genus one of the parts remains non-crossing as before, but the other has the requirement of being non-crossing when its chords are drawn in a surface of positive genus, with ends on the boundary of a disk in that surface.

These genus-g non-crossing chord diagrams, arising from the work in this chapter, seem completely unstudied in the literature. Some obvious questions arise about the enumeration of such objects. If $F_g(x)$ is the generating series for genus-g non-crossing chord diagrams, we would have the relations $[x^n]F_g(x) \leqslant [x^n]F_{g'}(x)$ whenever $g \leqslant g'$. We also know that the coefficients of $F_0(x)$ are the Catalan numbers and $\lim_{g\to\infty} F_g(x)$ is the generating function for all chord diagrams. It would be valuable to know a closed form for $F_g(x)$ in terms of g and x. It would also be valuable to know whether the genus-g non-crossing chord diagrams admit a characterization in terms of forbidden subdiagrams for every g. There are many variants of chord diagrams studied in the literature already, so it would also be valuable to know if there is a direct relationship with any of these.

The Quadrangulation Conjecture remains open. While new structure was elucidated by the series of bijections constructed in this thesis, there remains a problem of 'genus-reduction' whereby a quadrangulation in genus g must be made to correspond to a

set of maps of all genera from 0 through $g-1$, in addition to a map of genus g. We found some combinatorial suggestions that this also be done through the manipulation of one-face spanning submaps by re-expressing the coefficient-level formula in terms of the numbers $e_\gamma^T(\nu)$ of edges of a spanning one-face submap in genus γ with ν vertices. The nature of these manipulations remains elusive, however. Another task that remains is to relate the work in this document to the work in [2] which provides a bijection in genus 1. Our focus on spanning one-face submaps also aligns with the literature on so-called 'quasitrees' appearing in, for example, [22]. Work on quasitrees is very focused on a notion of 'partial duality' which may have a fruitful application here if explored in future work.

In chapter 3 we demonstrated that any two-regular graph G has at least $(n-2)!/4$ compatible cycles, i.e., cycles C for which the edge-disjoint union $G \cup C$ decomposes as an edge-disjoint union $C_1 \cup C_2$ of two cycles. If the cycles in G are all of even lengths, we demonstrated that this bound increases to $(n-2)!/2$. We additionally demonstrated that our proof of these results can be used to algorithmically construct compatible cycles in sufficient numbers for any 2-regular graph G.

We also found a connection between our results and some existing literature on genomic rearrangements in bioinformatics. We used some results from that literature to find an exact value for the number of compatible cycles to a graph consisting only of 2-cycles, in terms of the signed Hultman numbers $S_H^{\pm}(n/2-1,1)$.

The results of chapter 3 are the first step of two in a possible way of computing general Feynman integrals in terms of tree-level integrals in a large class of quantum field theories including Supersymmetric Yang-Mills theory. The second step, which remains to be completed, is to demonstrate that enough of the cycles compatible to a particular graph are orthogonal in the sense that a certain inner product in $\mathcal{M}_{0,n}$ computed in terms of them be zero.

References

[1] V. Bafna and P.A. Pevzner. Genome rearrangements and sorting by reversals. In *Proceedings of 1993 IEEE 34th Annual Foundations of Computer Science*, pages 148–157, 1993.

[2] Brown, Daniel. *Differential Equations and Depth First Search for Enumeration of Maps in Surfaces*. PhD thesis, 1999.

[3] Freddy Cachazo and Humberto Gomez. Computation of contour integrals on $\mathcal{M}_{0,n}$. *Journal of High Energy Physics*, 2016, 04 2016.

[4] Freddy Cachazo, Song He, and Ellis Yuan. Scattering equations and matrices: from einstein to yang-mills, dbi and nlsm. *Journal of High Energy Physics*, 2015, 12 2014.

[5] Freddy Cachazo, Song He, and Ellis Ye Yuan. Scattering equations and kawai-lewellen-tye orthogonality. *Phys. Rev. D*, 90:065001, Sep 2014.

[6] Freddy Cachazo, Song He, and Ellis Ye Yuan. Scattering of massless particles in arbitrary dimensions. *Phys. Rev. Lett.*, 113:171601, Oct 2014.

[7] Freddy Cachazo, Song He, and Ellis Ye Yuan. Scattering of massless particles: scalars, gluons and gravitons. *Journal of High Energy Physics*, 2014:33, July 2014.

[8] Freddy Cachazo, Song He, and Ellis Ye Yuan. Einstein-Yang-Mills scattering amplitudes from scattering equations. *Journal of High Energy Physics*, 2015:121, January 2015.

[9] Freddy Cachazo, Song He, and Ellis Ye Yuan. New double soft emission theorems. *Phys. Rev. D*, 92:065030, Sep 2015.

[10] Freddy Cachazo, Karen Yeats, and Samuel Yusim. Compatible cycles and CHY integrals. *Journal of High Energy Physics*, 2019(12):105, December 2019.

[11] Luigi Del Debbio. Quantum mechanics. https://www2.ph.ed.ac.uk/~ldeldebb/QM.html.

[12] R. Diestel. *Graph Theory: 5th edition*. Springer Graduate Texts in Mathematics. Springer-Verlag, 2017.

[13] Torsten Ekedahl, Sergei Lando, Michael Shapiro, and Alek Vainshtein. On hurwitz numbers and hodge integrals. *Comptes Rendus de l'Académie des Sciences - Series I - Mathematics*, 328(12):1175–1180, 1999.

[14] C. Godsil and G.F. Royle. *Algebraic Graph Theory*. Graduate Texts in Mathematics. Springer New York, 2013.

[15] Simona Grusea and Anthony Labarre. The distribution of cycles in breakpoint graphs of signed permutations. *Discrete Applied Mathematics*, 161(10):1448–1466, 2013.

[16] D. M. Jackson and T. I. Visentin. A character-theoretic approach to embeddings of rooted maps in an orientable surface of given genus. *Transactions of the American Mathematical Society*, 322(1):343–363, 1990.

[17] David Jackson, M. Perry, and T. Visentin. Factorisations for partition functions of random hermitian matrix models. *Communications in Mathematical Physics*, 179, 08 1997.

[18] David Jackson and T.I. Visentin. *An Atlas of the smaller maps in orientable and nonorientable surfaces*. 01 2000.

[19] D.M. Jackson and T.I. Visentin. A formulation for the genus series for regular maps. *Journal of Combinatorial Theory, Series A*, 74(1):14–32, 1996.

[20] D.M. Jackson and T.I. Visentin. A combinatorial relationship between eulerian maps and hypermaps in orientable surfaces. *Journal of Combinatorial Theory, Series A*, 87(1):120–150, 1999.

[21] Sergei Lando and Alexander Zvonkin. *Graphs on Surfaces and Their Applications*, volume 141. 01 2004.

[22] Iain Moffatt. Separability and the genus of a partial dual. *European Journal of Combinatorics*, 34(2):355–378, 2013.

[23] Stephen J. Parke and T. R. Taylor. Amplitude for n-gluon scattering. *Phys. Rev. Lett.*, 56:2459–2460, Jun 1986.

[24] Yuan, Ye. *Scattering Equations and S-Matrices*. PhD thesis, 2015.

[25] D. Zagier and J. Harer. The euler characteristic of the moduli space of curves. *Inventiones mathematicae*, 85:457–486, 1986.

[26] A. Zee. *Quantum Field Theory in a Nutshell*. Princeton University Press, 2010.